Neurobiology of Disease

Site-Specific Regulation of P2X7 Receptor Function in Microglia Gates Morphine Analgesic Tolerance

Heather Leduc-Pessah,[1,2] Nicholas L. Weilinger,[2,3] Churmy Y. Fan,[1,2] Nicole E. Burma,[1,2] Roger J. Thompson,[2,3] and Tuan Trang[1,2]

[1]Departments of Comparative Biology & Experimental Medicine, and Physiology & Pharmacology, [2]Hotchkiss Brain Institute, and [3]Department of Cell Biology and Anatomy, University of Calgary, Calgary, Alberta T2N 4N1, Canada

Tolerance to the analgesic effects of opioids is a major problem in chronic pain management. Microglia are implicated in opioid tolerance, but the core mechanisms regulating their response to opioids remain obscure. By selectively ablating microglia in the spinal cord using a saporin-conjugated antibody to Mac1, we demonstrate a causal role for microglia in the development, but not maintenance, of morphine tolerance in male rats. Increased P2X7 receptor (P2X7R) activity is a cardinal feature of microglial activation, and in this study we found that morphine potentiates P2X7R-mediated Ca^{2+} responses in resident spinal microglia acutely isolated from morphine tolerant rats. The increased P2X7R function was blocked in cultured microglia by PP2, a Src family protein tyrosine kinase inhibitor. We identified Src family kinase activation mediated by μ-receptors as a key mechanistic step required for morphine potentiation of P2X7R function. Furthermore, we show by site-directed mutagenesis that tyrosine ($Y_{382–384}$) within the P2X7R C-terminus is differentially modulated by repeated morphine treatment and has no bearing on normal P2X7R function. Intrathecal administration of a palmitoylated peptide corresponding to the $Y_{382–384}$ site suppressed morphine-induced microglial reactivity and preserved the antinociceptive effects of morphine in male rats. Thus, site-specific regulation of P2X7R function mediated by $Y_{382–384}$ is a novel cellular determinant of the microglial response to morphine that critically underlies the development of morphine analgesic tolerance.

Key words: ATP; microglia; opioid; P2X7; spinal cord; tolerance

Significance Statement

Controlling pain is one of the most difficult challenges in medicine and its management is a requirement of a large diversity of illnesses. Although morphine and other opioids offer dramatic and impressive relief of pain, their impact is truncated by loss of efficacy (analgesic tolerance). Understanding why this occurs and how to prevent it are of critical importance in improving pain therapies. We uncovered a novel site ($Y_{382–384}$) within the P2X7 receptor that can be targeted to blunt the development of morphine analgesic tolerance, without affecting normal P2X7 receptor function. Our findings provide a critical missing mechanistic piece, site-specific modulation by $Y_{382–384}$, that unifies P2X7R function to the activation of spinal microglia and the development of morphine tolerance.

Introduction

Opioids are essential for treating moderate to severe pain, but their effectiveness diminishes with repeated use and leaves patients without adequate pain control. This loss in pain-relieving effect is a cardinal feature of opioid analgesic tolerance and undermines the utility of opioids for long-term pain management. The development of opioid tolerance involves both peripheral and central mechanisms (Mayer et al., 1999; Zhou et al., 2010; Hutchinson et al., 2011; Iwaszkiewicz et al., 2013; Cai et al., 2016; Corder et al., 2017). Centrally, the spinal dorsal horn is a primary site of action for the analgesic effects of morphine and other

Received March 27, 2017; revised Sept. 3, 2017; accepted Sept. 8, 2017.

Author contributions: H.L.-P., R.J.T., and T.T. designed research; H.L.-P., N.L.W., C.Y.F., and N.E.B. performed research; H.L.-P., N.L.W., C.Y.F., and N.E.B. analyzed data; H.L.-P. and T.T. wrote the paper.

This work was supported by Grants from the Natural Sciences and Engineering Research Council of Canada (NSERC RGPIN418299) to T.T. and (NSERC RPGIN435762) to R.J.T.; the Canadian Institutes of Health Research (CIHR MOP133523), the Rita Allen Foundation/American Pain Society, and the Canada Foundation for Innovation to T.T.; an NSERC Graduate Scholarship to H.L-P.; an Alberta Innovates Health Solutions Graduate Scholarship to N.L.W. and H.L.-P.; an Eyes High University of Calgary scholarship to C.F.; and a Queen Elizabeth II and CIHR scholarship to N.E.B. We thank Dr. Yi Li for assistance with the behavioral studies; Dr. Francois Rassendren for generously providing the P2X7R plasmid; Drs. Christophe Altier, Robyn Flynn, and Frank Visser for assistance in generating the mutant P2X7R plasmid and BV2 cell PCR; Dr. Morley Hollenberg for discussions on peptide design; and Ms. Barbe Zochodne for comments on the paper.

The authors declare no competing financial interests.

Correspondence should be addressed to Dr. Tuan Trang, Departments of Comparative Biology & Experimental Medicine, and Physiology & Pharmacology, Hotchkiss Brain Institute, University of Calgary, 3330 Hospital Drive, Calgary, AB T2N 4N1, Canada. E-mail: trangt@ucalgary.ca.

DOI:10.1523/JNEUROSCI.0852-17.2017

 0270-6474/17/3710154-19$15.00/0

opioids, and in this region glia play a critical role in the cellular and behavioral corollary of opioid tolerance (Hutchinson et al., 2008; Mika et al., 2009; Zhou et al., 2010; Cai et al., 2016). In particular, microglia have emerged as key targets of opioid action, and in response to repeated opioid exposure, microglia shift toward a reactive phenotype. The shift toward a reactive microglial phenotype and the development of opioid tolerance are attenuated by treatment with nonselective glial inhibitors, such as minocycline, fluorocitrate, or propentofylline (Watkins et al., 2005; Sweitzer and De Leo, 2011; Wen et al., 2011). These inhibitors provided the first clues that glia are important modulators of opioid analgesia, but the key cellular substrates and processes that increase microglial reactivity in response to opioid treatment remain an important unresolved question.

Recent evidence indicates that ATP-gated P2X7 receptors (P2X7Rs) and P2X4 receptors (P2X4Rs) critically modulate the microglial response to opioid treatment. Specifically, P2X4R-mediated BDNF release from microglia is critical for opioid-induced hyperalgesia (a paradoxical increase in pain sensitivity; Ferrini et al., 2013), whereas P2X7R activation of pannexin-1 channels is differentially involved in opioid withdrawal (Burma et al., 2017a); however, neither of these mechanisms is required for opioid tolerance (Ferrini et al., 2013; Burma et al., 2017b). Evidence that P2X7R might be an important modulator of opioid tolerance came from recent observations that the loss in analgesia coincides with an increase in P2X7R protein, and that pharmacological blockade of P2X7R attenuates the loss in morphine antinociception (Zhou et al., 2010; Chen et al., 2012). However, the core mechanisms by which morphine modulates P2X7R activity to produce tolerance are not known. Here, we uncovered a novel mechanism through which morphine treatment potentiates P2X7R expression and function in microglia. This morphine-induced potentiation of P2X7R function is critically dependent on $Y_{382–384}$ within the P2X7R intracellular C-terminal domain. Our findings together provide a unifying explanation for how morphine engages P2X7R activity in microglia and its impact on morphine analgesia.

Materials and Methods

Animals

All experiments were approved by the University of Calgary Animal Care Committee and are in accordance with the guidelines of the Canadian Council on Animal Care. Male Sprague-Dawley rats (200–250 g) aged 6–8 weeks were purchased from Charles River Laboratories and housed under a 12 h light/dark cycle with *ad libitum* access to food and water.

Morphine treatment and nociceptive testing

Morphine sulfate (PCCA) was administered (15 mg/kg, i.p.) once a day over a period of 7 d. A morphine dose–response was performed on day 8. Thermal nociceptive threshold was assessed using the tail-flick test, with the application of an infrared thermal stimulus (Ugo Basile) to the ventral surface of the tail (D'Amour and Smith, 1941) and latency to remove tail from the stimulus was recorded; a maximum of 10 s was used to prevent tissue damage. Mechanical nociceptive threshold was measured using the Randall–Selitto paw-pressure test via an Analgesy-Meter that applied a linearly increasing force to the hindpaw (Ugo Basile; McNaull et al., 2007). The weight in grams eliciting a paw flexion or vocalization was defined as the mechanical nociceptive threshold. To avoid tissue damage, a maximum of 500 g was used as a cutoff (Zhao et al., 2012). Nociceptive measurements were taken before and 30 min after morphine injection, and the values normalized to daily baseline measurements. A day 1 time course of morphine-induced antinociception was performed at 30, 60, and 180 min after the first acute injection of morphine. In a subset of experiments on day 8, a morphine dose–response was performed to determine morphine potency (ED_{50}). At 30 min intervals, rats were given ascending doses of morphine (2.5, 5, 15, 30, 50, 80 mg/kg) until a maximal level of antinociception was reached in both the tail-flick and paw-pressure tests.

Intrathecal drug administration

Drugs were administered by intrathecal injection under light anesthetic with 1% isoflurane (v/v) as described previously by De la Calle and Paíno (2002). Unless otherwise stated, intrathecal injections were delivered 30 min before intraperitoneal morphine or saline injections. Nociceptive testing was performed before the intrathecal injection and 30 min after morphine or saline treatment. Drugs included A740003 (0.1 nmol; Sigma-Aldrich), Mac-1 saporin and saporin (15 μg; Advanced Targeting Systems), and palmitoylated peptides (20 nmol; Genemed Synthesis). All compounds were administered intrathecally in a 10 μl volume, including vehicle control (saline or saline with 0.2% DMSO).

Mac1-saporin. Saporin-conjugated antibody to Mac1 (Mac1-saporin; 15 μg), or unconjugated saporin (15 μg) control, was administered by intrathecal injection. To examine the importance of spinal microglia in the development of morphine tolerance, intrathecal Mac1-saporin was administered once daily for 3 d before initiating morphine treatment. To examine the role of spinal microglia in the tonic expression of morphine tolerance, intrathecal Mac1-saporin injections were administered to rats with established morphine tolerance on days 6–8. Nociceptive testing in Mac1-saporin or saporin alone treated rats was performed 30 min after morphine or saline treatment. Motor coordination in Mac1-saporin and saporin alone treated rats was examined using the accelerating rotarod test (IITC Life Science).

Palmitoylated peptides. $P2X7R_{356–371}$ (NTYASTCCRSRVYPSC, rat), $P2X7R_{356–371}$ (NTYSSAFCRSGVYPYC, mouse), $P2X7R_{379–389}$ (VNEYYYRKKCE, rat/mouse), inactive $P2X7R_{Y379–389F}$ (VNEFFFRKKCE, rat/mouse), $P2X7R_{546–556}$ (RHCAYRSYATW, rat), $P2X7R_{546–556}$ (RHRAYRCYATW, mouse), and $P2X7R_{586–595}$ (GQYSGFKYPY, rat/mouse) were synthesized by Genemed Synthesis. The amino acid composition of each peptide was based on P2X7R protein sequences obtained from GenBank (*Mus musculus*; AAI41121.1) and NCBI (*Rattus norvegicus*; NP_062129.1). Peptides targeting regions of mouse, or both rat and mouse, P2X7R were used in BV2 cells and peptides targeting regions of the rat, or both rat and mouse, P2X7R were used *in vivo*. Each palmitoylated peptide covered a unique tyrosine-containing region(s) within the P2X7R C-terminal domain, and was comparable in terms of molecular weight, isoelectric point, charge, length, and solubility.

Microglia cell cultures

Primary microglia culture from adult rat spinal cord for calcium imaging. Microglia were acutely isolated from the adult rat spinal cord as previously described (Yip et al., 2009). Briefly, morphine tolerant and saline control treated rats deeply anesthetized with 4% isoflurane were perfused with heparinized (1 U/ml) 0.9% saline. The spinal cord was rapidly isolated by hydraulic extrusion and placed in ice-cold Hibernate A media supplemented with B27 and glutamine (0.5 mM). Spinal cords were cut into 0.5 mm longitudinal sections using a McIlwain tissue chopper and transferred to 6 ml Hibernate A media containing papain (12 mg, 15–23 U/mg protein) and incubated for 30 min at 30°C. Samples were triturated using a 1 ml pipette, centrifuged at 397 × *g* for 5 min at room temperature, and the resulting pellet was again suspended in 1 ml fresh DFP (DMEM + GlutaMax-1 media [Gibco] and 1% penicillin-streptomycin [Gibco]) media. To remove debris, samples were filtered through a 100 μm cell strainer (BD Biosciences) and rinsed with 1 ml DFP medium. Cells were plated onto 25 mm diameter glass coverslips coated with poly-L-lysine and maintained in DFP within an incubator at 37°C with 5% CO_2 and 95% O_2. After 24 h, cells were prepared for Ca^{2+} imaging experiments.

Primary microglia culture from adult rat spinal cord for flow cytometry. Morphine tolerant and saline control treated rats were deeply anesthetized with 4% isoflurane and perfused with PBS. The spinal cord was rapidly isolated by hydraulic extrusion and placed in HBSS. Spinal cords were cut into smaller sections and then transferred to a 70 μm cell strainer in DMEM supplemented with 2% FBS and 10 mM HEPES. To deplete myelin, tissue was filtered through strainer, mixed with isotonic

Percoll, and Percoll (density 1.08) was underlain before centrifugation (1200 × *g*, 20°C, 30 min). Cells accumulating at the interface between layers were removed, rinsed, and stained for flow cytometry.

Primary microglia culture from postnatal rats. Primary microglia cultures were prepared as described by Trang et al. (2009). In brief, mixed glial culture was isolated from postnatal day (P)1–P3 Sprague-Dawley rat cortex or rat spinal cord and maintained for 10–14 d in DMEM containing 10% FBS and 1% penicillin-streptomycin at 37°C with 5% CO_2. Microglia separated from the mixed culture by gentle shaking were plated and treated daily with morphine (1 μM) or saline. After 5 d, microglia were prepared for Western blot analysis and Ca^{2+} imaging experiments.

BV2 microglia culture. BV2 microglia (CLS, Catalog #ATL03001; RRID:CVCL_0182) were maintained in DMEM (Invitrogen) containing 10% FBS, 1% penicillin-streptomycin at 37°C with 5% CO_2. Cells were treated daily with morphine (1 μM) and one of the following drugs: CTAP (5 μM; Sigma-Aldrich), *genistein* (10 μM; Sigma-Aldrich), *genistin* (10 μM; Sigma-Aldrich), PP2 (10 μM; Sigma-Aldrich), PP3 (*10* μM; Calbiochem), KBSrc4 (5 μM; Tocris Bioscience), palmitoylated peptides (10 μM; Genemed Synthesis), LPS-RS (10, 100 ng/ml; InvivoGen) or with DAMGO (1 μM; Tocris Bioscience). After 5 d of drug treatment, BV2 cells were prepared for Western blot analysis, Ca^{2+} imaging, or whole-cell recordings. Control cultures were treated with saline and/or one of the above drugs in the absence of morphine once daily for 5 d.

Calcium imaging

Cells were incubated for 30 min with the fluorescent Ca^{2+} indicator dye Fura-2 AM (2.5 μM; Invitrogen) in extracellular solution (ECS) containing the following (in mM): 140 NaCl, 5.4 KCl, 1.3 $CaCl_2$, 10 HEPES, and 33 glucose, pH 7.35, osmolarity 315–320 mOsm (Trang et al., 2009). All experiments were conducted at room temperature using an inverted microscope (Nikon Eclipse Ti C1SI Spectral Confocal) and the fluorescence of individual microglia was recorded using EasyRatioPro software (PTI). Excitation light was generated from a xenon arc lamp and passed in alternating manner through 340 or 380 nm bandpass filters (Omega Optical). The 340:380 fluorescence ratio was calculated after baseline subtraction.

Whole-cell patch-clamp recordings

BV2 cells were visualized via differential interface contrast imaging with a TCS SP5 II microscope (Leica) and acquired with an IR-1000 infrared camera (DAGE-MTI). Whole-cell patch-clamp recordings were obtained using borosilicate glass microelectrodes (Sutter Instrument) with a tip resistance of 4–7 MΩ using a P-1000 Flaming/Brown Micropipette Puller (Sutter Instrument) and filled with a CsCl intracellular solution containing the following (in mM): 130 CsCl, 10 NaCl, 10 EGTA, 0.1 $CaCl_2$, 4 K_2-ATP, and 0.3 Na_3-GTP, and buffered with 10 mM HEPES. Cells were voltage-clamped at −60 mV and continuously superfused at a rate of 1–2 ml/min with ECS containing the following (in mM): 140 NaCl, 5.4 KCl, 2 $CaCl_2$, 25 HEPES, 33 glucose, 1 $MgCl_2$, pH 7.35, osmolarity 345–355 mOsm, and bubbled with 95% O_2/5% CO_2. BzATP (1 mM) was puffed for 5 s onto cells at a distance of >200 μm. Membrane currents were recorded in episodic sweeps with BzATP applied every 60 s. BzATP-evoked responses between 3 and 10 min of recording were analyzed for peak amplitude and area under the curve.

Flow cytometry

Primary mixed neuron-glia culture was isolated from rat spinal cord and maintained for 7 d as described above. Acutely isolated adult spinal cords were extracted and cells were collected as described above. For flow cytometric analysis, cells were washed and collected in PBS containing 10% FBS, filtered through a 100 μm cell strainer, and stained with fluorophore-conjugated antibodies P2X7R-ATTO 633 (1:250; Alomone Labs) and cluster of differentiation molecule 11b (CD11b)/c-PE (1:500; eBioscience) for 45 min at 4°C with rotation. Cell fluorescence was measured by an Attune Acoustic Focusing Cytometer (Applied Biosystems) with the following threshold and voltage settings: forward scatter threshold, 400; FSC voltage, 3300; SSC voltage, 2700; BL2 voltage, 1800; RL1 voltage, 1100. Live single-cell population was gated using forward and side scatter plot. CD11b and P2X7R-positive staining were gated using BL2 and RL1 intensities respectively, in single stained cells compared with unstained cells.

Fluorescent-activated cell sorting and PCR

Acutely isolated adult rat spinal cords were collected and processed as described above and labeled with α-rat CD11b/c-PE (1:1000; eBioscience). Cells positive for CD11b were gated and sorted using a BD FACSAria III cell sorter into a collection tube for mRNA extraction at the Flow Cytometry Core Facility. mRNA was extracted from CD11b-positive cells using Phenol/chloroform extraction and converted to cDNA using reverse transcriptase. Primers were designed to amplify ~100 bp fragments of CD11b (forward: CTGCCTCAGGGATCCGTAAAG; reverse: CCTCTGCCTCAGGAATGACATC), GFAP (forward: CGCTTCCTGGAACAGCAAAA; reverse: CCCGAAGTTCTGCCTGGTAAA), MAP2 (forward: CAAAAGATCAGAAAGACTGGTTCATC; reverse: CAGCTAAACCCCATTCATCCTT), and μ-receptor (forward: CAGCTGCCTGAATCCAGTTCTT; reverse: CGAGTGGAGTTTTGCTGTTCG) mRNA.

Immunohistochemistry

Rats were anesthetized with pentobarbital (Bimeda-MTC Animal Health) and perfused transcardially with 4% paraformaldehyde (w/v) in 0.1 M phosphate buffer, pH 7.4. The spinal lumbar segment was dissected, postfixed overnight in 4% paraformaldehyde, transferred to 30% sucrose, embedded in OCT, and then sectioned at 30 μm thickness using a cryostat. Free-floating spinal cord sections were incubated overnight at 4°C in mouse α-CD11b antibody (1:150; CBL1512 EMD, Millipore), rabbit α-P2X7R antibody (1:150; APR-008, Alomone Labs), rabbit α-μ-receptor antibody (1:500; AOR-011, Alomone Labs), rabbit α-Ki67 antibody (1:500; ab16667, Abcam), rabbit α-Iba1 antibody (1:1000; 019-19741, Wako). Sections were incubated at 20–25°C with fluorochrome-conjugated secondary antibodies (1:1000; Cy3- and Cy5-conjugated AffiniPure Donkey anti-mouse or anti-rabbit IgG, Jackson ImmunoResearch). Images were obtained using a Nikon Eclipse Ti (C1SI Spectral Confocal) or a Nikon A1-R multiphoton microscope. Images were acquired using E2-C1 software and converted using Nis Elements imaging software. Quantification of CD11b-IR mean intensity and percentage area positive labeling was performed using ImageJ (NIH). As previously described by Riazi et al. (2008), activated microglia from Iba1-labeled tissue were distinguished by the presence of fewer short and thick processes as well as an amoeboid, hypertrophic appearance. All images were coded and the experimenter assessing microglial morphology was blinded to the treatment conditions.

P2X7R cell-surface biotinylation

BV2 microglia cell cultures were maintained and treated as described previously. Before collection, adherent cells were incubated with 1 mg/ml EZ-link Sulfo-NHS-SS-Biotin (Thermo Scientific) in HBSS on ice for 1 h to bind cell-surface proteins. This reaction was quenched by incubation with 100 mM glycine. Cell-surface protein samples were normalized to total protein content and incubated with High Capacity Neutravidin Agarose Resin (Thermo Scientific) for 1.5 h at 4°C with rotation. Beads were washed and again suspended in loading buffer and P2X7R protein levels measured by Western blotting.

Western blotting

Microglia in culture were harvested in 200 μl lysis buffer containing 50 mM TrisHCl, 150 mM NaCl, 10 mM EDTA, 0.1% Triton-X, 5% Glycerol, protease inhibitors, and phosphatase inhibitors. Rat spinal cord tissue was rapidly isolated and homogenized in RIPA buffer containing the following: 50 mM TrisHCl, 150 mM NaCl, 2 mM EDTA, 0.1% SDS, 1% NP-40, 0.5% sodium deoxycholate, 1 mM Na_3VO_4, 1 U/ml aprotinin, 20 μg/ml leupetin, and 20 μg/ml pepstatin A. Both microglia and spinal cord samples were incubated on ice for 30 min before centrifugation at 12,000 rpm at 4°C for 30 min. Total protein was measured using a Bio-Rad RC DC Protein Assay Kit or Pierce BCA Protein Assay Kit (Thermo Scientific). Samples were heated at 95°C for 10 min in loading buffer (350 mM Tris, 30% glycerol, 1.6% SDS, 1.2% bromophenol blue, 6% β-mercaptoethanol), electrophoresed on a precast SDS gel (4–12% TrisHCl, Bio-Rad) or on a 10% polyacrylamide gel, and transferred onto nitrocellulose membrane. The membrane was probed with rabbit

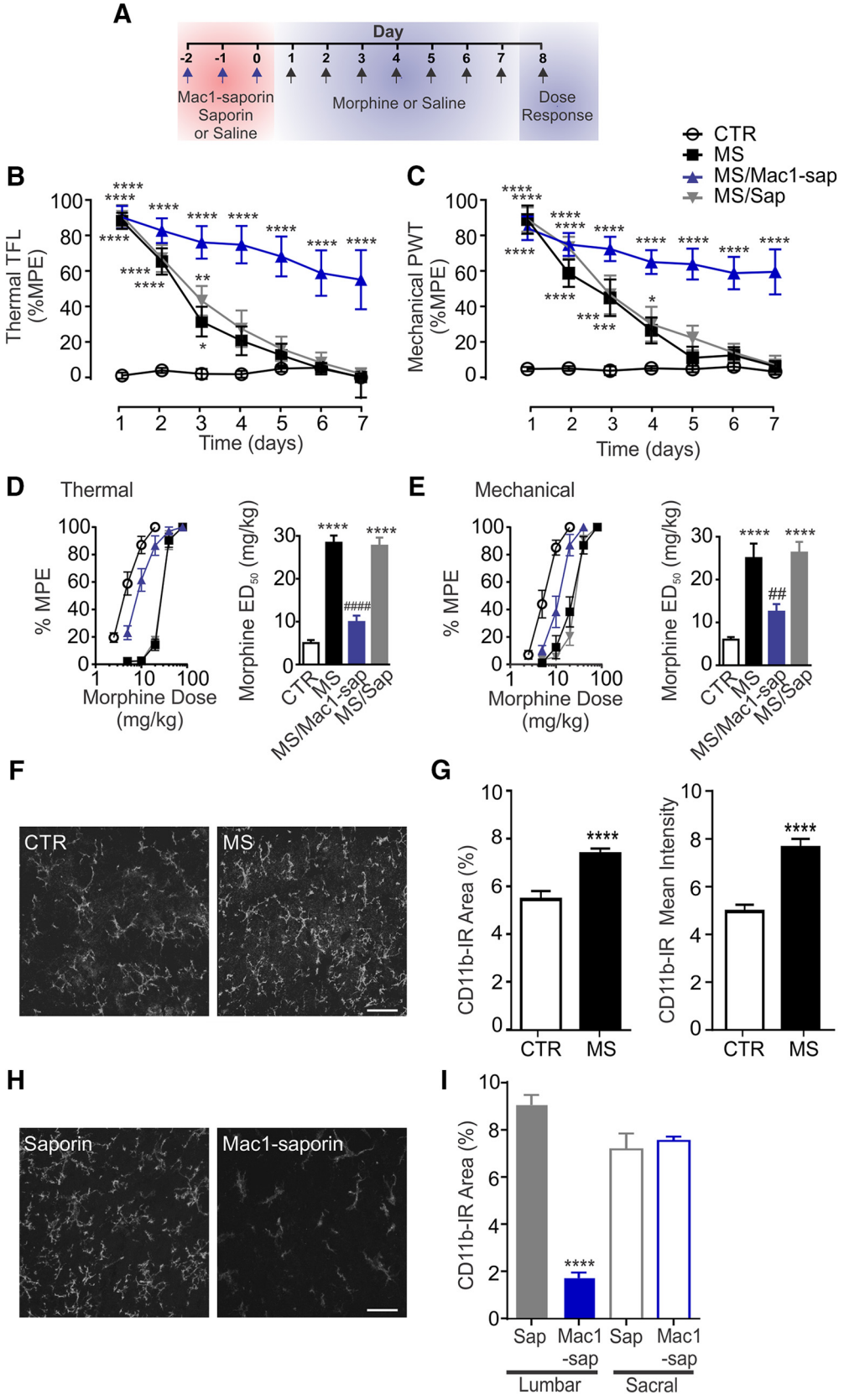

Figure 1. Development of morphine tolerance depends on spinal microglia. ***A***, Schematic of drug administration paradigm. Intrathecal injections of Mac1-saporin (15 μg; $n = 8$) or saporin ($n = 6$) were administered before daily morphine sulfate (MS; 15 mg/kg; $n = 7$) or saline (CTR; $n = 7$) treatment. ***B***, ***C***, Morphine antinociception was assessed using (***B***) thermal tail-flick (10 s cutoff) and (***C***) mechanical paw-pressure (500 g cutoff). Latency to withdraw from stimulus, tail-flick latency (TFL) and paw withdrawal thresholds (PWT), are reported as a percentage of the maximum possible effect (MPE). ****$p < 0.0001$, ***$p < 0.001$, **$p < 0.01$, *$p < 0.05$. Repeated-measures two-way ANOVA (***B***, interaction: $F_{(18,168)} = 4.5$; time: $F_{(6,168)} = 24.4$; treatment: $F_{(3,168)} = 93.3$; ***C***, interaction: $F_{(18,168)} = 5.1$; time: $F_{(6,168)} = 25.9$; treatment: $F_{(3,168)} = 100.3$), Dunnett's *post hoc* test. ***D***, ***E***, Morphine dose–response curves and median (*Figure legend continues.*)

α-P2X7R antibody (1:1000; APR008, Alomone Labs), mouse α-β-Actin (1:2000; A5316, Sigma-mAldrich), rabbit α-μ-receptor antibody (1:500; AOR-011, Alomone), mouse α-c-Src (1:500; sc-8056, Santa Cruz Biotechnology), or rabbit α-p-SrcTyr416 (1:500; D49G4, Cell Signaling Technology). Membranes were washed in TBST (20 mM Tris, 137 mM NaCl, 0.05% Tween20) and incubated for 1 h at room temperature in fluorophore-conjugated secondary antibodies (1:5000; anti-rabbit and anti-mouse-conjugated IR Dyes, Mandel Scientific). Membranes were imaged and quantified using the LICOR Odyssey Clx Infrared Imaging System (Mandel Scientific). Band intensity was quantified using ImageJ, normalized to β-actin and expressed relative to control samples. All quantification was done using original images, for representative images brightness and contrast were adjusted equally across all lanes using Corel Draw.

Coimmunoprecipitation

BV2 cell lysates were prepared as described above and incubated with rabbit α-c-src antibody (1 μg/100 μg protein) at 4°C overnight. Samples were then incubated with Protein A and Protein G-Sepharose beads 1:1 (GE Healthcare) at 4°C for 2 h. Immunoprecipitates were then washed with lysis buffer, suspended in Laemmli sample buffer, and boiled for 5 min. Proteins were resolved by Western blotting and probed for Src as described above.

P2X7R constructs

Plasmid constructs (p1275 Flag) expressing *p2rx7* coding sequence under EcoRV promoter were obtained from the laboratory of Dr. Francois Rassendren (Montpellier University, France). The construct was modified to encode an mCherry protein downstream of the *p2rx7* gene. Y382-384A mutations were introduced by site-directed mutagenesis using Q5 High-Fidelity DNA Polymerase (New England BioLabs), and constructs verified by DNA sequencing. Plasmids were transfected into 1321N1 human astrocytoma cells using Lipofectamine-2000 (Invitrogen). After transfection, cells were maintained in DMEM supplemented with 10% FBS and treated with saline or morphine (1 μM). Transfected cells were identified by mCherry expression and BzATP-evoked P2X7R-mediated calcium responses were measured by calcium imaging.

Statistics

All data are presented as the mean ± SEM. Statistical analyses of the results were performed using a Student's *t* test, one-way ANOVA (Dunnett or Sidak *post hoc* test), two-way ANOVA (Dunnett, Sidak, or Tukey *post hoc* test), or two-way repeated-measures ANOVA (Dunnett *post hoc* analysis).

Results

To investigate the mechanisms underlying opioid tolerance, we treated rats with morphine sulfate (15 mg/kg of body weight, i.p.) once daily for 7 d (Fig. 1*A*). Morphine antinociception was measured by testing thermal tail-flick latency and mechanical paw withdrawal threshold 30 min after injection (Fig. 1*B*,*C*). Treatment with morphine induced a significant increase in thermal and mechanical threshold on day 1. However, this antinociceptive effect was reduced within 3 d of treatment (Fig. 1*B*,*C*). By day 5, morphine had no effect on either thermal or mechanical threshold, indicating the rats were tolerant to the antinociceptive effects of morphine (Fig. 1*B*,*C*). In addition to the progressive decline in morphine antinociception, a key feature of tolerance is the reduction in analgesic potency. To assess morphine potency, we performed a dose–response, which entailed administering ascending doses of morphine every 30 min until a maximal antinociceptive effect was achieved in both the thermal and mechanical tests. Rats treated with morphine for 7 d required substantially higher doses of morphine, compared with morphine naive (saline treated) rats, to achieve a maximal antinociceptive response (Fig. 1*D*,*E*). The requirement for higher doses in morphine treated rats was reflected by a rightward shift in the morphine dose–response curve and a significant fivefold increase in median effective dose (ED_{50}; Fig. 1*D*,*E*). Thus, daily morphine treatment results in a loss of analgesic potency, a finding that is consistent with the development of morphine tolerance.

Spinal microglia are critically involved in the development of morphine tolerance

Microglia are key opioid targets and studies have established that spinal microglial activity opposes opioid analgesia in the CNS (Song and Zhao, 2001). We found a significant increase in CD11b immunoreactivity within the spinal dorsal horn of morphine-treated rats compared with saline-treated rats; this increase in CD11b expression is a cellular correlate of microglial activation and indicates that spinal microglia respond to morphine treatment (Fig. 1*F*,*G*). Therefore, we examined whether spinal microglia may differentially underlie the development and/or tonic expression of morphine tolerance. To delineate whether spinal microglia are required for the development of tolerance, we depleted microglia in the spinal dorsal horn using intrathecal injections of Mac1-saporin (15 μg; Fig. 1*A*). This depletion was specifically localized to the spinal lumbar (L3–L5) site of injection (Fig. 1*H*,*I*), and did not alter baseline nociceptive responses to thermal or mechanical stimuli (Fig. 2*F*,*G*). Mac1-saporin also did not alter the peak antinociceptive response to a single dose of morphine, or affect motor performance in the accelerating rotarod test (Fig. 2*H–J*). However, we found that Mac1-saporin, but not saporin alone (15 μg), attenuated the loss in morphine antinociception (Fig. 1*B*,*C*) and prevented the reduction in morphine potency (Fig. 1*D*,*E*), indicating that spinal microglia are required for the development of morphine tolerance. To determine whether microglia are also necessary for the tonic expression of tolerance, we tested the effects of intrathecal administration of Mac1-saporin (15 μg) in rats with established analgesic tolerance after 6–8 d of morphine treatment (Fig. 2*A*). We found that depleting microglia in the spinal cord of morphine tolerant rats neither reversed the loss in morphine antinociception (Fig. 2*B*,*C*), nor restored morphine potency in the thermal tail-flick test or the mechanical paw withdrawal test (Fig. 2*D*,*E*). Therefore, we conclude that spinal microglia are causally involved in the development, but not the tonic expression, of morphine tolerance.

Morphine potentiates P2X7R activity in adult spinal microglia

ATP-gated P2X7Rs critically modulate the activity of microglia (Monif et al., 2009). Within the spinal dorsal horn, multiple stud-

←

(*Figure legend continued.*) effective dose (ED_{50}) values as measured on day 8 following 7 d morphine or saline treatment. Measures are reported as percentage of the maximum possible effect. ***D***, CTR: 5.0 ± 0.7 mg/kg; MS: 28.4 ± 1.7 mg/kg; MS/Mac1-sap: 9.9 ± 1.5 mg/kg; MS/Sap: 27.7 ± 1.9 mg/kg (CTR vs MS: $p < 0.0001$; MS vs MS/Mac1-saporin: $p < 0.0001$; CTR vs MS/saporin: $p < 0.0001$). ***E***, CTR: 6.0 ± 0.6 mg/kg; MS: 25.0 ± 3.4 mg/kg; MS/Mac1-sap: 12.5 ± 1.8 mg/kg; MS/Sap: 26.3 ± 2.5 mg/kg (CTR vs MS: $p < 0.0001$; MS vs MS/Mac1-saporin: $p = 0.002$; CTR vs MS/saporin: $p < 0.0001$). ****$p < 0.0001$ compared with CTR; ####$p < 0.0001$, ##$p < 0.01$ compared with MS; one-way ANOVA (***D***: $F_{(3,24)} = 64$; ***E***: $F_{(3,24)} = 18$; Sidak's *post hoc* test). ***F***, Representative images of CD11b expression in the spinal lumbar dorsal horn following 7 d of saline or morphine treatment (60×). Scale bar, 50 μm. ***G***, Quantification of CD11b-immunoreactivity (IR) by percentage of total area, and by mean intensity of CD11b labeling (CTR, $n = 9$; MS, $n = 12$ spinal cord sections). Unpaired two-tailed *t* test (%Area: $t = 4.7$, df = 19, $p < 0.0001$; intensity: $t = 5.5$, df = 19, $p < 0.0001$). ****$p <$ 0.0001 compared with control group. ***H***, Representative images of CD11b expression in the spinal lumbar dorsal horn following 3 d of saporin or Mac1-saporin (15 μg) injections (60×). Scale bar, 50 μm. ***I***, Mac1-saporin reduced CD11b immunoreactivity is localized to the lumbar (L4–L5; Mac1-sap, $n = 8$; Sap, $n = 8$) site of injection. CD11b immunoreactivity was not affected caudal (S3–S4; Mac1-sap, $n = 9$; Sap, $n = 7$) to the site of injection. One-way ANOVA ($F_{(3,28)} = 67$; lumbar: $p < 0.0001$; sacral: $p = 0.7829$), Sidak's *post hoc* test. ****$p < 0.0001$ compared with Sap. All data represent mean ± SEM.

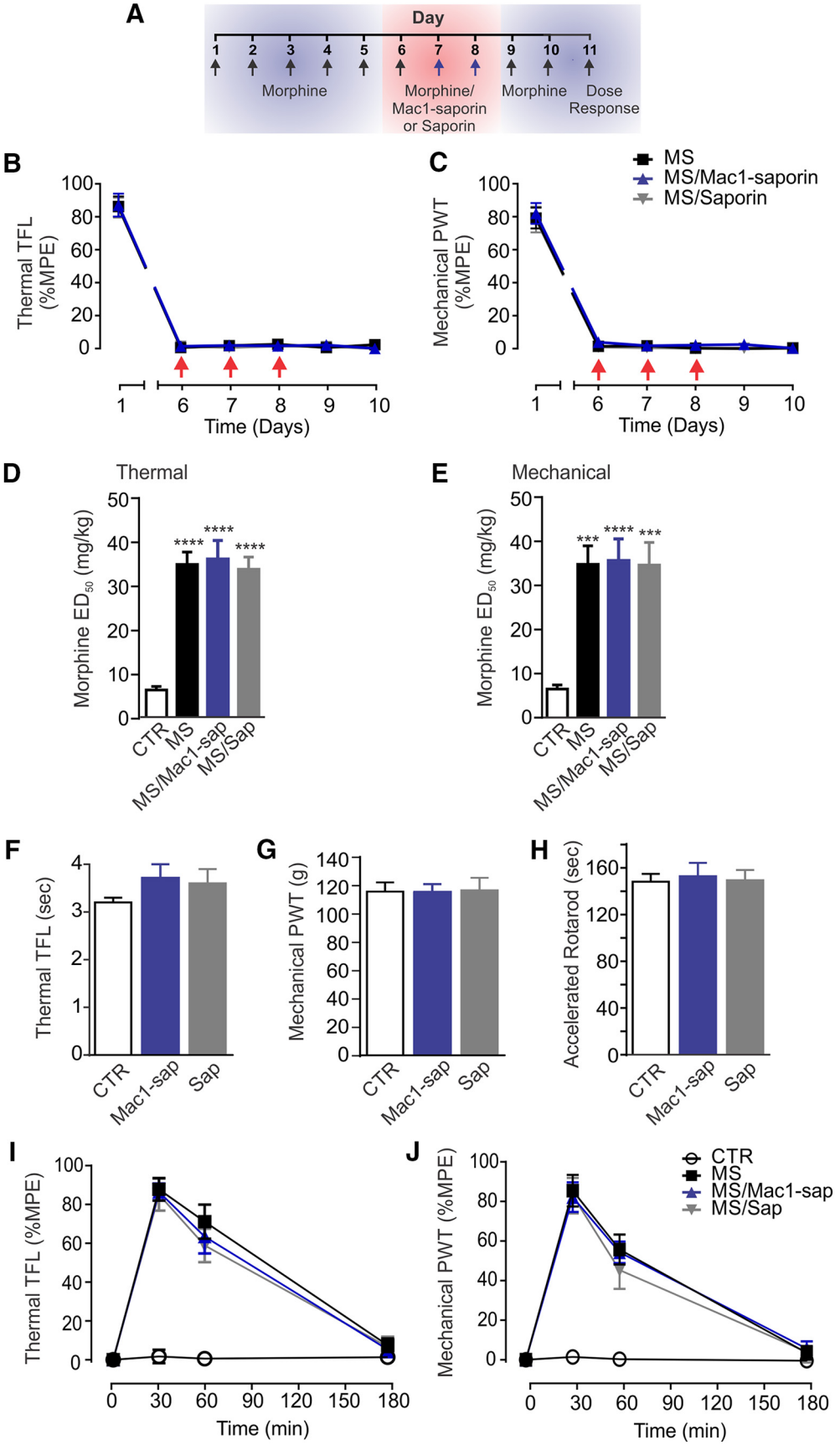

Figure 2. Spinal microglia do not critically underlie maintenance of morphine tolerance. ***A***, Schematic of drug administration paradigm used to examine spinal microglia involvement in the ongoing expression of morphine tolerance. Intrathecal Mac1-sap ($n = 7$), sap ($n = 7$), or CTR ($n = 7$) injections were administered on days 6–8 to rats with established morphine tolerance. ***B***, ***C***, MS antinociception was assessed daily using the (***B***) thermal tail-flick test and (***C***) mechanical paw-pressure test. Tail-flick latencies (TFLs) and paw(*Figure legend continues.*)

ies show that these receptors are predominantly expressed on microglia (Jarvis, 2010; Chen et al., 2012; Volonté et al., 2012). To confirm the localization of P2X7Rs, we isolated spinal cords from P1–P3 rat pups and performed flow cytometric analysis of mixed cultures labeled with CD11b and P2X7R (Fig. 3*A*,*B*). This analysis in primary cells revealed two distinct cell populations: a CD11b-positive population with positive P2X7R labeling, and a CD11b-negative population (i.e., neurons and astrocytes) with weak P2X7R labeling (Fig. 3*A*). Mean P2X7R immunofluorescence revealed a marked rightward shift in P2X7R signal in the CD11b-positive population compared with the CD11b-negative population (Fig. 3*B*). These findings confirm there is a high density of P2X7R expression on CD11b-positive cells, which in the spinal cord are microglia.

In morphine tolerant rats, there was a significant increase in total P2X7R protein expression within the lumbar spinal cord (Fig. 3*C*). We examined whether this increase in P2X7R occurred on microglia by acutely isolating the spinal cords of rats treated with saline or morphine for 7 d (Fig. 3*D*–*H*). P2X7R density (as measured by mean P2X7R intensity per cell) was significantly higher on CD11b-positive cells compared with CD11b-negative cells (Fig. 3*D*,*E*). In morphine tolerant rats, there was a significant increase in P2X7R density in CD11b-positive cells, but no change in P2X7R density in CD11b-negative cells (Fig. 3*D*). Thus, repeated morphine treatment differentially upregulates P2X7R expression on microglia. Antibody specificity for flow cytometric analysis was determined by comparison to unstained control cells and nonspecific IgG or secondary only controls (Fig. 3*F*–*H*).

As our findings indicate that P2X7Rs are localized on spinal microglia, we questioned whether morphine treatment affects the activity of these receptors. To assess P2X7R cation channel activity, we acutely isolated adult primary cells from the spinal cord of naive and morphine tolerant rats. Adult spinal microglia were identified using CD11b labeling (Fig. 3*I*) and cells were loaded with fura-2, a Ca^{2+}-indicator dye, and exposed to BzATP (100 μM), a potent P2X7R agonist with partial activity at P2X1 and P2Y1 (Bianchi et al., 1999). Exposure to BzATP induced a rise in intracellular Ca^{2+} concentration, and this rise was significantly greater in microglia isolated from the spinal cord of morphine tolerant rats compared with saline-treated rats (Fig. 3*J*,*K*). Because P2X1R is rapidly desensitized (Rettinger and Schmalzing, 2004), and treatment with a selective P2X7R antagonist A740003 abolished the BzATP-evoked responses (see Fig. 5*G*,*H*), we conclude that morphine treatment potentiates endogenous P2X7R activity in resident spinal microglia.

To target spinal P2X7Rs, rats were treated with intrathecal injections of a selective P2X7R antagonist A740003 (Honore et al., 2006). When administered with daily morphine treatment, A740003 significantly attenuated the decline in morphine antinociception (Fig. 4*A*,*B*), and prevented the loss in morphine potency (Fig. 4*C*,*D*). By contrast, in rats with established morphine tolerance intrathecal injections of A740003 did not restore the antinociceptive effects of morphine (Fig. 4*E*,*F*). Together, our results indicate that spinal P2X7Rs critically contribute to the development but not the ongoing expression of morphine tolerance. We cannot exclude the potential contribution of A740003 inhibition of P2X7Rs on neurons and astrocytes in the development of morphine tolerance *in vivo*. Nonetheless, we have shown that in response to morphine treatment, P2X7R expression and function are selectively increased in microglia. Therefore, given the localization of P2X7Rs on spinal microglia, we infer that the increase of P2X7R expression and activity in microglia may contribute to the development of morphine tolerance.

Morphine signals through μ-receptors to modulate P2X7R expression and activity

To examine whether morphine acts directly on microglia, and to determine the key intracellular mechanisms that modulate P2X7R function, we used a BV2 microglial cell line and primary microglial cultures that respond to morphine and express both P2X7R and μ-receptor (Fig. 5*A*,*B*). We confirmed that acutely isolated adult spinal microglia also coexpress P2X7R and μ-receptor (Fig. 5*A*), and that fluorescent-activated cell sorted CD11b-positive cells express μ-receptor mRNA (Fig. 5*C*). We determined in BV2 and primary microglia that 5 d morphine treatment caused a concentration-dependent increase in total P2X7R protein expression (Fig. 5*D*,*E*), and that this increase was concomitant with a potentiation of P2X7R-mediated Ca^{2+} responses (Fig. 5*F*,*G*). To assess P2X7R function more directly, we transiently puffed BzATP (1 mM, 5 s) onto BV2 cells and recorded electrophysiological changes using whole-cell patch-clamp. As with Ca^{2+} responses, P2X7R-mediated inward currents were increased by morphine treatment (Fig. 5*H*) and both were blocked by A740003 (Fig. 5*G*,*H*). We confirmed that the increase in P2X7R expression and activity elicited *in vivo* were recapitulated in primary microglia culture following repeated morphine treatment (Fig. 5*E*,*F*). Because cell yield is prohibitively low in primary microglia cultures, and given that BV2 microglia are fully competent to respond to morphine, we conducted subsequent *in vitro* experiments using the BV2 microglia cell line.

Because morphine is a potent μ-receptor agonist, we asked whether the increase in P2X7R protein expression and activity were dependent on μ-activity. To examine μ-receptor involvement, microglia were cotreated with morphine and CTAP, a selective μ-receptor antagonist, or with DAMGO, a synthetic opioid peptide that selectively activates μ-receptors (Onogi et al., 1995). In the presence of CTAP, neither P2X7R protein expression (Fig. 6*A*) nor P2X7R activity (Fig. 6*D*,*E*) was affected by morphine treatment. Total μ-receptor protein expression in BV2 microglia was also not altered by morphine treatment (Fig. 6*B*). By contrast, repeated exposure to DAMGO increased P2X7R protein expression, whereas DPDPE and U69593, selective δ- and κ-receptor agonists, respectively, had no effect on P2X7R levels (Fig. 6*C*). Treatment with DAMGO also potentiated P2X7R-mediated currents, demonstrating that μ-receptor activation is sufficient to enhance P2X7R function in microglia (Fig. 6*D*,*E*).

It has been suggested that the effects of morphine on microglia may involve Toll-like receptor 4 (TLR4; Hutchinson et al., 2010).

←

(*Figure legend continued.*) withdrawal thresholds (PWTs) are presented as percentage of maximum possible effect (MPE). ***D***, ***E***, Morphine median effective dose (ED50) values following 10 d of treatment. ***D***, CTR: 6.2 ± 0.81 mg/kg; MS: 34.82 ± 2.84 mg/kg; MS/Mac1-Sap: 36.05 ± 4.25 mg/kg; MS/Sap: 33.75 ± 2.75 mg/kg (CTR vs MS: $p < 0.0001$; CTR vs MS/Mac1-saporin: $p < 0.0001$; CTR vs MS/saporin: $p < 0.0001$). ***E***, CTR: 6.51 ± 0.94 mg/kg; MS: 34.98 ± 4.2 mg/kg; MS/Mac1-Sap: 35.79 ± 4.95 mg/kg; MS/Sap: 34.8 ± 5.14 mg/kg (CTR vs MS: $p = 0.0002$; CTR vs MS/Mac1-saporin: $p < 0.0001$; CTR vs MS/saporin: $p = 0.0004$), one-way ANOVA ($F_{(3,24)} = 24$; $F_{(3,24)} = 11.8$), Dunnett's *post hoc* test. ***F–J***, Intrathecal injections of Mac1-saporin, saporin, or saline were administered for 3 d before testing or to morphine (MS) treatment. ***F–H***, Baseline nociceptive responses in the (***F***) thermal tail-flick test (CTR = 3.2 ± 0.1 s; Mac1-sap = 3.7 ± 0.3 s; Sap = 3.6 ± 0.3 s), (***G***) mechanical paw-pressure test (CTR = 115.7 ± 6.5 g; Mac1-sap = 115 ± 6.0 g; Sap = 116.7 ± 8.8 g), and (***H***) locomotor performance in the accelerated rotarod test. One-way ANOVA ($F_{(2,18)} = 1.1$; $F_{(2,18)} = 0.01$; $F_{(2,18)} = 0.07$), no significance. ***I***, ***J***, Time course to first MS injection over 180 min. TFLs and PWTs are presented as percentage of MPE. Antinociceptive response to a single systemic injection of MS (15 mg/kg) was not affected by Mac1-sap ($n = 8$), sap ($n = 6$), or CTR treatment. All data represent mean ± SEM. ****$p < 0.0001$, ***$p < 0.001$ compared with CTR.

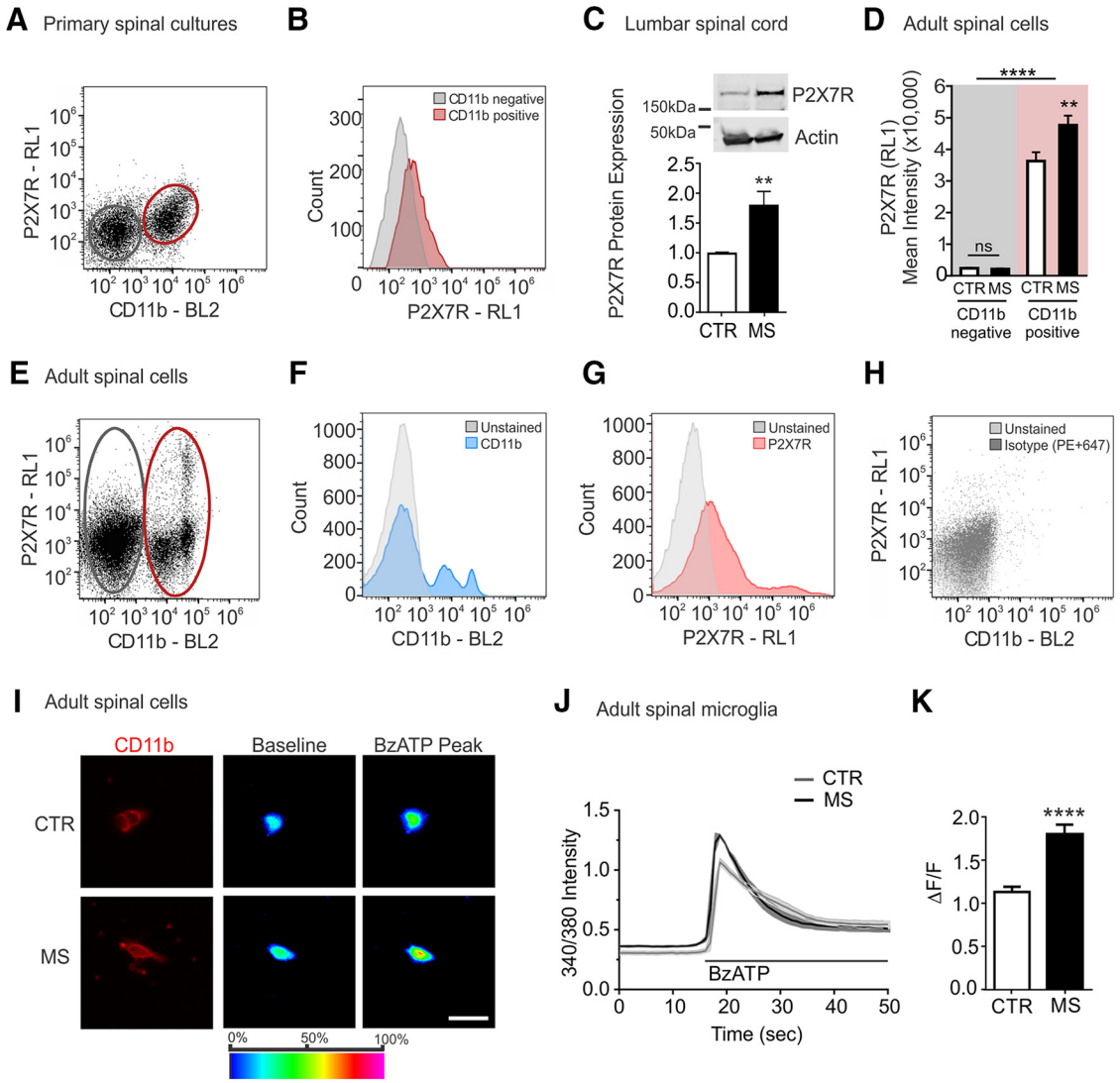

Figure 3. Spinal microglial P2X7R expression and activity are increased in morphine tolerant rats. ***A***, ***B***, Primary rat spinal cord cultured cells. ***A***, Representative dot plot of primary spinal cord cultures imaged using flow cytometry labeled for CD11b (BL2 area, *x*-axis) and P2X7R (RL1 area, *y*-axis). ***B***, Histogram of P2X7R (RL1) intensity in CD11b-positive and CD11b-negative populations. ***C***, P2X7R protein levels as measured by Western blot in spinal cord homogenates isolated from rats treated with MS ($n = 13$) or CTR ($n = 13$) for 7 d. Unpaired two-tailed *t* test ($t = 3.3$, df $= 24$, $p = 0.0027$). ***D–K***, Spinal cord cells were acutely isolated from adult rats that had received 7 d of systemic MS or CTR treatment. ***D***, Quantification of P2X7R (RL1) mean intensity in CD11b-negative and-positive populations from control and morphine-treated animals using flow cytometry. Two-way ANOVA (interaction: $F_{(1,16)} = 7.7$; CD11b +ve/−ve: $F_{(1,16)} = 366.9$; treatment: $F_{(1,16)} = 7.2$), Sidak's *post hoc* test, main effect of population $p < 0.0001$; CD11b-negative CTR vs MS: $p = 0.9969$; CD11b-positive CTR vs MS: $p = 0.0027$. ***E***, Representative dot plot of acutely isolated adult spinal cord cells from control-treated animals imaged using flow cytometry and labeled for CD11b (BL2 area, *x*-axis) and P2X7R (RL1 area, *y*-axis). CD11b-negative and CD11b-positive populations used for analysis are circled in black and red, respectively. ***F***, Histogram of CD11b (BL2) single stained control overlaid with unstained cells in adult spinal cord cells. ***G***, Histogram of P2X7R (RL1) single stained control overlaid with unstained cells in adult spinal cord cells. ***H***, Dot plot of primary spinal cultures labeled with IgG-PE and anti-rabbit IgG-647 as controls overlaid with unstained cells. ***I***, Representative image of adult spinal cord cells labeled with α-rat CD11b antibody to identify microglia. Representative images of microglia loaded with the Ca^{2+} indicator dye fura-2 AM in the 340 nM Ca^{2+} bound channel (40×). Scale bar, 20 μm. ***J***, Representative Ca^{2+} tracings from microglia loaded with the Ca^{2+} indicator dye fura-2 AM. ***K***, Peak rise in intracellular [Ca^{2+}] evoked by BzATP. BzATP-evoked (100 μM) rise in intracellular [Ca^{2+}] was greater in microglia isolated from MS- ($n = 42$ cells) compared with CTR- ($n = 38$ cells) treated rats. Unpaired two-tailed *t* test ($t = 5.3$, df $= 20$, $p < 0.0001$). All data represent mean ± SEM. ****$p < 0.0001$, **$p < 0.01$.

To address the potential contribution of TLR4 in morphine potentiation of P2X7R function, we tested in cultured microglia the effects of a potent TLR4 antagonist, LPS-RS (lipopolysaccharide from *Rhodobacter sphaeroides*). Treatment with LPS-RS across a range of concentrations failed to block the morphine induced potentiation of P2X7R cation channel function or the increase in P2X7R protein expression (Fig. 6*F*,*G*). Our results are consistent with increasing evidence for a divergence of μ-receptor and TLR4 actions in microglia (Fukagawa et al., 2013; Stevens et al., 2013; Mattioli et al., 2014; Skolnick et al., 2014) and collectively indicate that the actions of morphine on P2X7R do not depend on TLR4. Thus, we conclude that μ-receptor activation increases the expression and activity of P2X7R autonomously in microglia.

Morphine potentiation of P2X7R activity is dependent on Src kinase

We questioned whether morphine treatment augments P2X7R activity in microglia by a protein kinase dependent mechanism. As an initial screen for potential kinase regulation of P2X7Rs, we used the broad-spectrum tyrosine kinase inhibitor genistein (10 μM; Levitzki and Gazit, 1995) that blocked the morphine potentiation of P2X7R-mediated Ca^{2+} responses (Fig. 7*A*). By

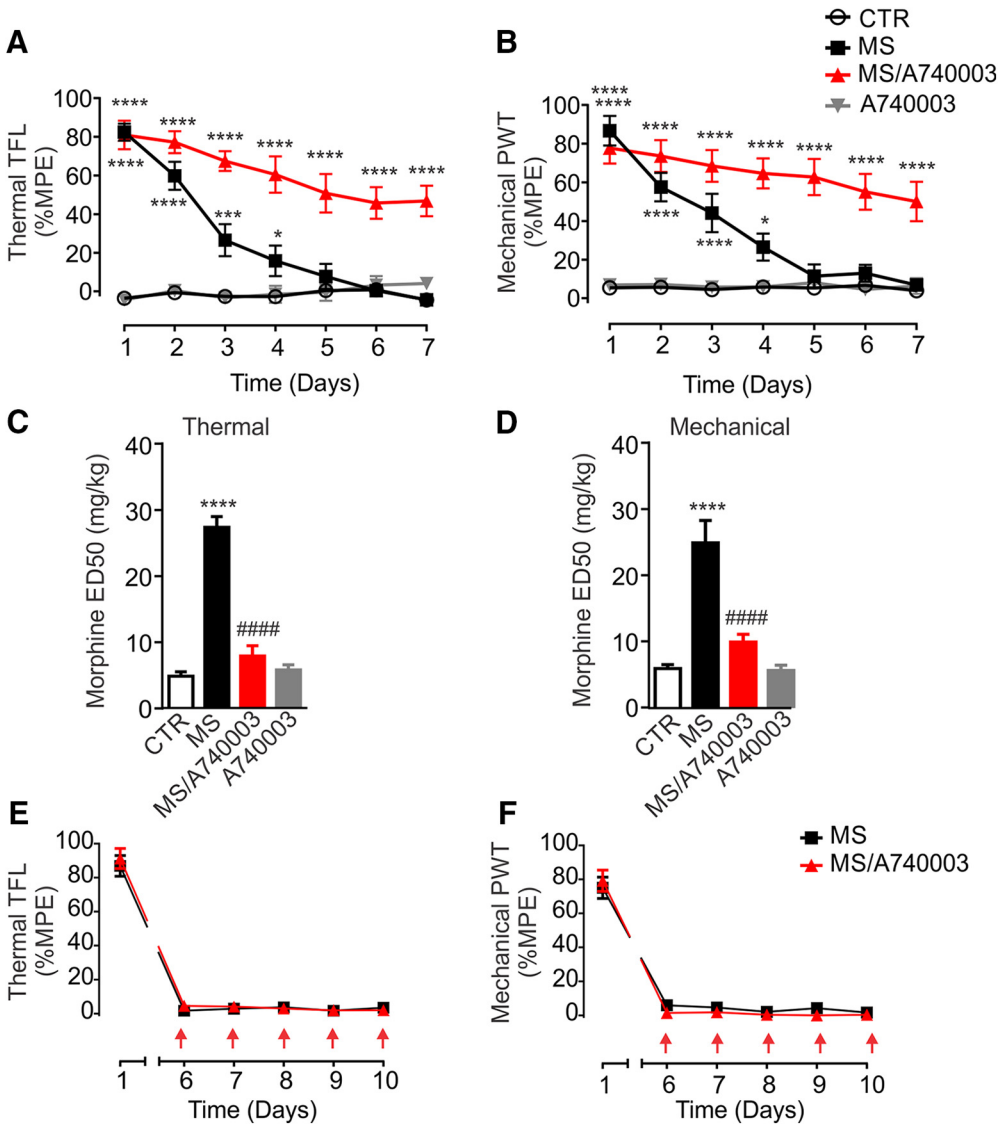

Figure 4. Spinal P2X7Rs are critically involved in the development of morphine tolerance. ***A–D***, Effects of intrathecal injections of A740003 (0.1 nmol), a selective P2X7R antagonist, on the development of morphine tolerance. ***A***, Thermal and (***B***) mechanical nociceptive threshold in CTR- ($n = 7$), MS- ($n = 7$), MS/A740003- ($n = 7$), and A740003- ($n = 6$) treated rats. Latency to withdraw from stimulus, tail-flick latency (TFL) and paw withdrawal thresholds (PWTs), are reported as a percentage of the maximum possible effect (MPE). ****$p < 0.0001$, ***$p < 0.001$, *$p < 0.05$, repeated-measures two-way ANOVA (***A***: interaction: $F_{(18,161)} = 8.7$; time: $F_{(6,161)} = 15.8$; treatment: $F_{(3,161)} = 201.7$; ***B***, interaction: $F_{(18,161)} = 5.4$; time: $F_{(6,161)} = 10.6$; treatment: $F_{(3,161)} = 155.3$), Dunnett's *post hoc* test. ***C***, ***D***, Morphine ED_{50} values following 7 d of treatment. ****$p < 0.001$ compared with CTR; ####$p < 0.0001$ compared with MS, one-way ANOVA (***C***: $F_{(3,23)} = 72.5$; ***D***: $F_{(3,23)} = 22.5$), Sidak's *post hoc* test. ***C***, CTR: 5.0 ± 0.7 mg/kg; MS: 28.4 ± 1.7 mg/kg; MS/A740003: 8.2 ± 1.6 mg/kg; A740003: 6.0 ± 0.8 mg/kg (CTR vs MS: $p < 0.0001$; MS vs MS/A740003: $p < 0.0001$). ***D***, CTR: 6.0 ± 0.6 mg/kg; MS: 25.0 ± 3.4 mg/kg; MS/A740003: 10.0 ± 1.2 mg/kg; A740003: 5.7 ± 0.8 mg/kg (CTR vs MS: $p < 0.0001$; MS vs MS/A740003: $p < 0.0001$). ***E***, ***F***, Effects of intrathecal injections of A740003 (0.1 nmol) on MS antinociception in rats with established tolerance. ***E***, Thermal and (***F***) mechanical nociceptive threshold was measured and is reported as a percentage of the MPE. A740003 was administered on days 6–10 with MS (MS, $n = 5$; MS/A740003, $n = 5$). All data represent mean ± SEM.

contrast, treatment with the inactive analog genistin (10 μM) had no effect on the increase in P2X7R function (Fig. 7*A*). We next tested a more selective protein tyrosine kinase inhibitor PP2 that suppresses the Src family of kinases. Treatment with PP2 (10 μM) prevented the morphine-induced increase in P2X7R-mediated Ca^{2+} responses (Fig. 7*A*,*B*) and currents (Fig. 7*C*,*D*), whereas the structurally similar but inactive analog PP3 (10 μM) had no effect on P2X7R function (Fig. 7*A*,*D*). From these findings, we conclude that the potentiation of P2X7R function by morphine critically depends on protein tyrosine kinase activity: specifically, we determined that P2X7R-mediated currents and Ca^{2+} responses in microglia are increased by Src family kinases.

Based on the pharmacological profiles of the inhibitors tested we deduced that the effects are mediated by Src family kinases, which is comprised of nine non-receptor tyrosine kinases. In our search for the critical kinase involved in morphine upregulation of P2X7R activity, we identified Src kinase (also known as c-src) as a key candidate because it is highly expressed in microglia, its activity is associated with microglia pain signaling, and previous studies have established a link between μ-receptor signaling and c-Src activation (Zhang et al., 2009, 2013; Rivat et al., 2014). We asked whether Src activity is affected by repeated morphine treatment, and examined this by first measuring the level of Src phosphorylation at tyrosine 416 (Y416), which is located within the activation loop of the kinase. Phosphorylation of this residue (pY416) is required for full activity of Src, and is a surrogate marker of Src kinase activation (Brown and Cooper, 1996). To assess whether morphine induces Src kinase activation, we im-

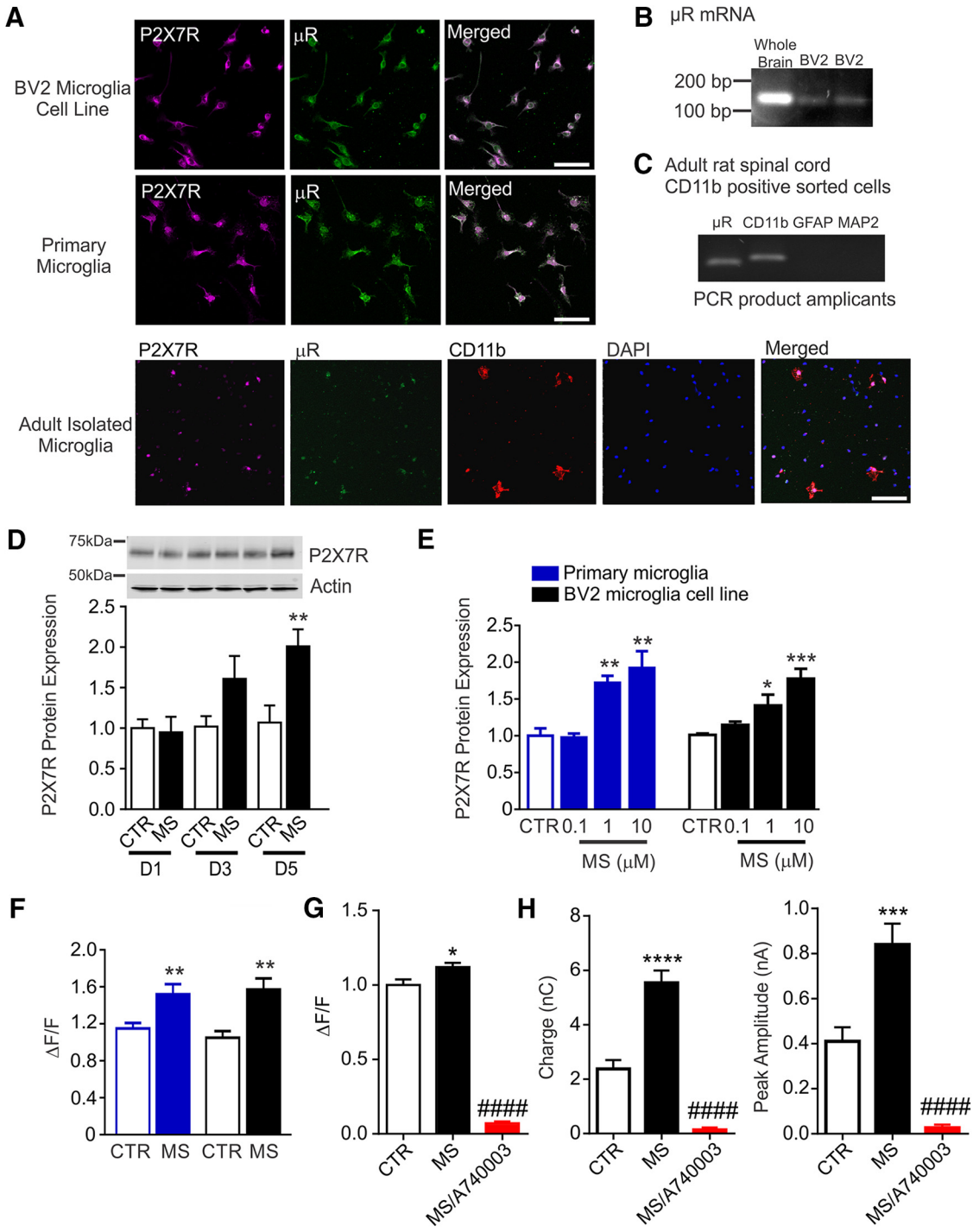

Figure 5. P2X7R expression and function are increased with repeated morphine in primary and BV2 microglia cultures. ***A***, P2X7Rs and μ-receptors (μR) are expressed on BV2 microglial cell line, primary microglia cultures isolated from P1–P3 rat brain and acutely isolated adult spinal microglia. ***B***, PCR products in whole mouse brain and BV2 microglia amplified with primers targeting μ-receptor mRNA. ***C***, Fluorescent-activated cell sorted microglia from adult rat spinal cord. PCR primers targeting CD11b, GFAP, MAP2, and μ-receptor mRNA amplifying 100 bp bands were used to amplify cDNA and products were run on a DNA gel. ***D***, Western blot analysis of P2X7R protein levels in BV2 cells after one, three, and five daily treatments with morphine (MS, $n = 5$). Two-way ANOVA (interaction: $F_{(1,24)} = 3.3$; treatment: $F_{(1,12)} = 9.4$; days: $F_{(2,24)} = 4.2$; D5 CTR vs MS: $p = 0.0074$), Sidak's *post hoc* test. ***E***, Five days of morphine (MS) produced a dose-dependent increase in P2X7R protein in primary and BV2 microglia (Primary; $n = 4$; BV2, $n = 6$). One-way ANOVA (Primary: $F_{(3,12)} = 12.8$; BV2: $F_{(3,19)} = 10.9$), Dunnett's *post hoc* test (Primary: CTR vs 1 μM MS: $p = 0.0076$; CTR vs 10 μM MS: $p = 0.0012$; BV2: CTR vs 1 μM MS: $p = 0.0229$; CTR vs 10 μM MS: $p = 0.0001$). $^{***}p < 0.001$, $^{**}p < 0.01$, $^{*}p < 0.05$ compared with CTR. ***F***, Peak rise in intracellular [Ca^{2+}] evoked by BzATP (100 μM; $n = 18, 22, 30, 42$). Unpaired two-tailed *t* tests (Primary: $t = 2.8$, df = 38, $p = 0.0085$; BV2: $t = 3.8$, df = 70, $p = 0.0012$). $^{**}p < 0.01$ compared with CTR. ***G***, ***H***, A740003, a P2X7R antagonist, (10 μM) was applied to the recording solution 10 min before and throughout Ca^{2+} imaging or whole-cell patch-clamp recordings. ***G***, A740003 blocked BzATP-evoked rise in intracellular [Ca^{2+}] (CTR, $n = 37$; MS, $n = 109$; MS/A740003, $n = 39$ cells). One-way ANOVA ($F_{(2,182)} = 263.7$), Sidak's *post hoc* test (CTR vs MS: $p = 0.0229$; MS vs MS/A740003: $p < 0.0001$). ***H***, A740003 reduced BzATP-evoked inward current (charge) and decreased peak amplitude. CTR and MS groups same as shown in Figures 6*E*, 7*D*, and 8*C*. MS/A740003 experimental group represent $n = 4$ cells. One-way ANOVA ($F_{(2,17)} = 42$; $F_{(2,20)} = 20.9$), Sidak's *post hoc* test (Charge: CTR vs MS: $p < 0.0001$; MS vs MS/A740003: $p < 0.0001$; Peak: CTR vs MS: $p = 0.0010$; MS vs MS/A740003: $p < 0.0001$). Quantification of P2X7R and μR protein levels were normalized to actin and represent change from the control group. All data represent mean ± SEM. $^{****}p < 0.0001$, $^{***}p < 0.001$, $^{**}p < 0.01$, $^{*}p < 0.05$ compared with CTR; $^{\#\#\#\#}p < 0.0001$, $^{\#\#\#}p < 0.001$, $^{\#\#}p < 0.01$ compared with MS.

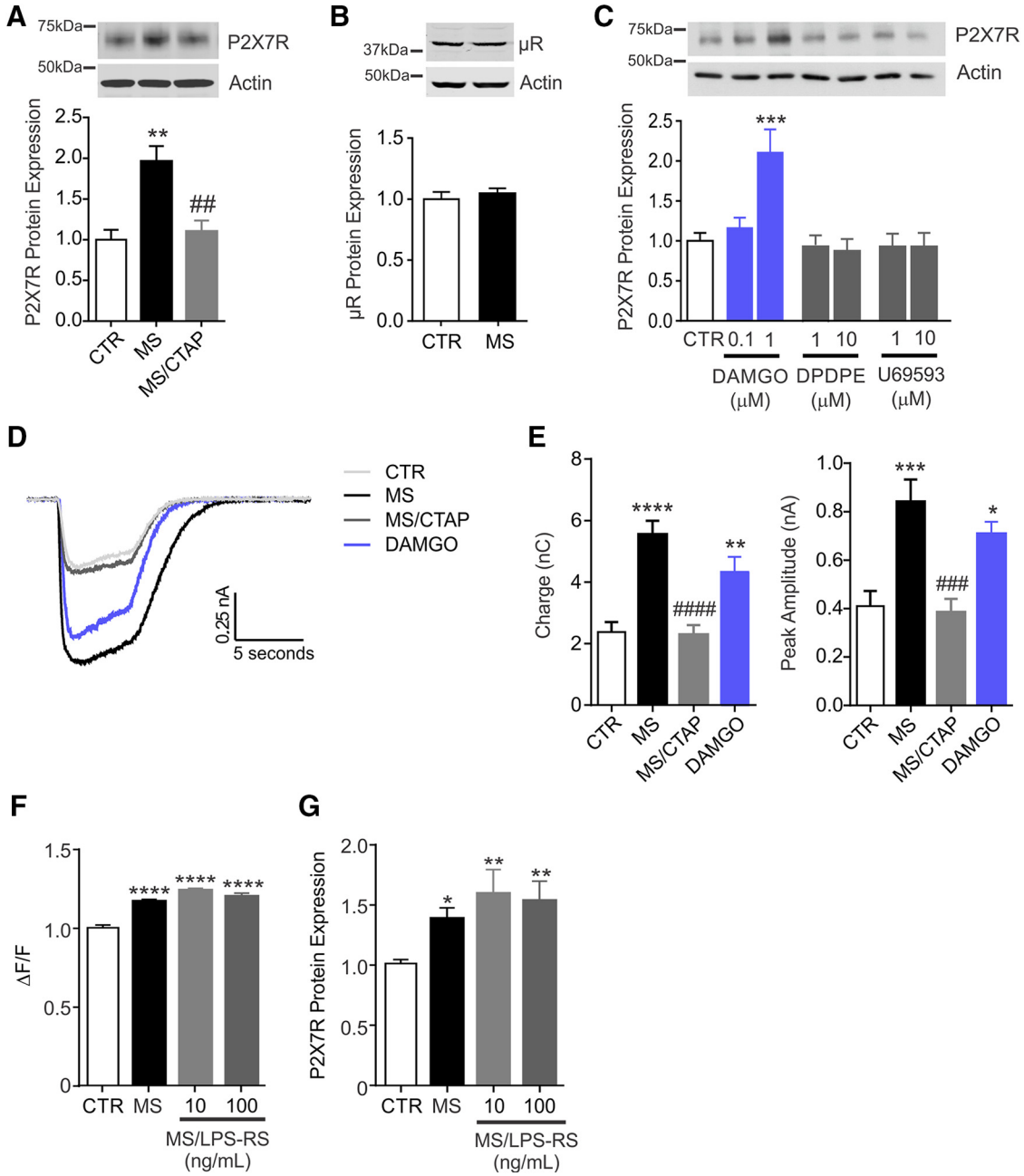

Figure 6. Morphine upregulation of P2X7R expression and function is mediated by μ-receptors (μRs). ***A–E***, BV2 cultured microglia were treated for 5 d with morphine (MS; 1 μM), PBS as a control (CTR), DAMGO (0.1 or 1 μM) a selective μR agonist, or selective δ and κ agonists. Antagonists were coadministered daily with morphine. ***A***, Morphine upregulation of P2X7R protein levels was blocked by CTAP (5 μM), a selective μR antagonist ($n = 4$). One-way ANOVA ($F_{(2,9)} = 12.2$), Sidak's *post hoc* test (CTR vs MS: $p = 0.0046$; MS vs MS/CTAP: $p = 0.0091$)b]. ***B***, Total μR protein expression in BV2 microglia was unchanged following MS or CTR treatment ($n = 4$). Unpaired two-tailed t test ($t = 0.6$, df $= 6$), not significant. ***C***, P2X7R protein expression as assessed by Western blotting following treatment with DAMGO (μR selective agonist), DPDPE (δ-receptor selective agonist), or U69593 (κ-receptor selective agonist; $n = 5$). One-way ANOVA ($F_{(6,21)} = 6.5$), Dunnett's *post hoc* test. (CTR vs 1 μM DAMGO: $p = 0.0009$). ***D***, Representative BzATP-evoked currents from whole-cell patch-clamp recordings of BV2 microglia. ***E***, Quantification of total charge (area under the curve) and peak amplitude for BzATP-evoked intracellular currents in BV2 microglia ($n = 9, 8, 7, 8$). CTR and MS groups same as shown in Figures 5*H*, 7*D*, and 8*C*. One-way ANOVA ($F_{(3,27)} = 14.9$; $F_{(3,30)} = 10.5$), Sidak's *post hoc* test (Charge: CTR vs MS: $p < 0.0001$; MS vs MS/CTAP: $p < 0.0001$; CTR vs DAMGO: $p = 0.0051$; Peak: CTR vs MS: $p = 0.0003$; MS vs MS/CTAP: $p = 0.0005$; CTR vs DAMGO: $p = 0.0133$). ***F***, ***G***, BV2 microglia were treated with CTR or MS (1 μM) for 5 d. LPS-RS (10 or 100 ng/ml) was coapplied with MS. ***F***, LPS-RS did not block the morphine-induced potentiation of BzATP-evoked calcium responses ($n \sim 250$–350 cells; 10 plates). One-way ANOVA ($F_{(4,1306)} = 50.8$), Sidak's *post hoc* test ($p < 0.0001$). ***G***, LPS-RS did not block morphine-induced increase in total P2X7R protein expression in BV2 microglia ($n = 11, 11, 6, 6$). One-way ANOVA ($F_{(3,30)} = 6.0$), Sidak's *post hoc* test (CTR vs MS: $p = 0.0296$; CTR vs MS/LPS-RS 10 ng/ml: $p = 0.0034$; CTR vs MS/LPS-RS 100 ng/ml: $p = 0.0089$). Quantification of P2X7R and μR protein levels were normalized to actin and represent change from the control group. All data represent mean ± SEM. ****$p < 0.0001$, ***$p < 0.001$, **$p < 0.01$, *$p < 0.05$ compared with CTR; ####$p < 0.0001$, ###$p < 0.001$, ##$p < 0.01$ compared with MS.

munoprecipitated Src from BV2 microglial lysates with a pan anti-Src antibody, and then probed with an antibody specific for pY416. We found that repeated morphine treatment increased the level of phospho-Src without changing the total expression of Src protein (Fig. 7*E*). Thus, repeated or sustained morphine exposure causes Src kinase activation in microglia.

We then examined whether the activation of Src was μ-receptor dependent. To test this, microglia in culture were treated with

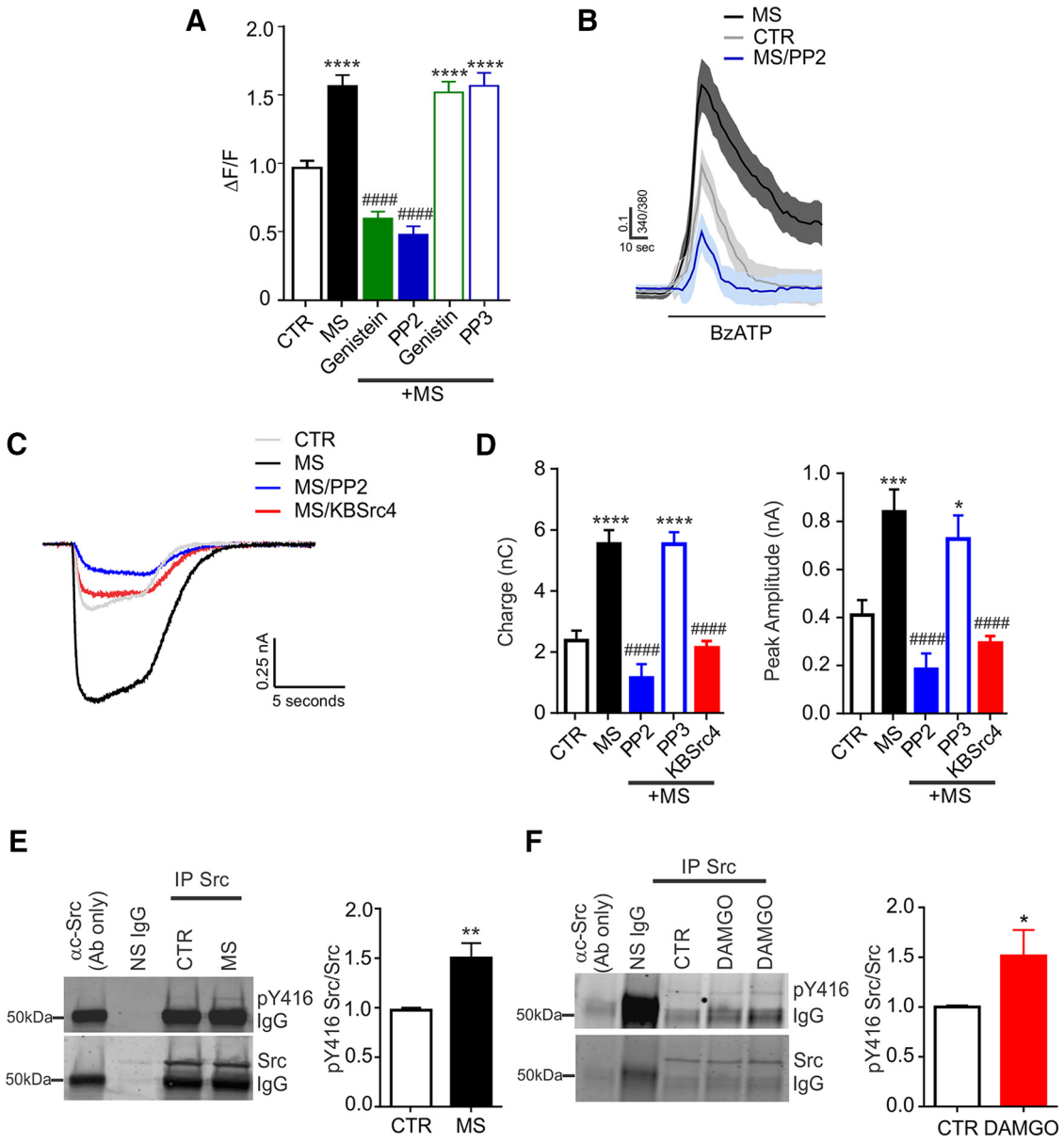

Figure 7. Morphine potentiation of P2X7R activity depends on Src kinase. ***A***, Average $\Delta F/F$ of single-cell BzATP-evoked responses in BV2 microglia expressed relative to CTR. Cells were treated with MS (1 μM) and genistein or genistin (10 μM), PP2, or PP3 (10 μM) for 5 d before imaging ($n = 30-42$ cells/group). One-way ANOVA ($F_{(5,214)} = 52.4$), Sidak's *post hoc* test ($p < 0.0001$). ***B***, Average of five BzATP-evoked [Ca^{2+}] responses for CTR, MS, and MS/PP2. ***C***, Representative tracings of the BzATP-evoked inward current in BV2 cells treated with MS (1 μM), MS + PP2 (10 μM), or MS + the src antagonist, KBSrc4 (5 μM), or CTR. ***D***, Average charge and peak amplitude for BzATP-evoked currents from BV2 microglia ($n = 9, 8, 6, 8, 9$). CTR and MS groups same as shown in Figures 5*H*, 6*E*, and 8*C*. One-way ANOVA ($F_{(4,34)} = 30.2$; $F_{(4,37)} = 13.6$), Sidak's *post hoc* test (Charge: CTR vs MS: $p < 0.0001$; MS vs MS/PP2: $p < 0.0001$; CTR vs MS/PP3: $p < 0.0001$; MS vs MS/KBSrc4: $p < 0.0001$; Peak: CTR vs MS: $p = 0.0006$; MS vs MS/PP2: $p < 0.0001$; CTR vs MS/PP3: $p < 0.0171$; MS vs MS/KBSrc4: $p < 0.0001$). ***E***, ***F***, Total src (c-src) was IP from BV2 microglia treated with MS (***E***) or DAMGO (***F***). The IP fraction was probed for phosphorylation of the active site of src kinase (pY416). pY416 src is normalized to levels of total src and expressed relative to CTR. ***E***, ($n = 8$) Unpaired two-tailed *t* test ($t = 3.4$, df = 14, $p = 0.0072$). ***F***, ($n = 9, 6$) Unpaired two-tailed *t* test ($t = 2.5$, df = 13, $p = 0.0283$). All data represent mean ± SEM. ****$p < 0.0001$, ***$p < 0.001$, **$p < 0.01$ *$p < 0.05$ compared with CTR; ####$p < 0.0001$ compared with MS.

DAMGO for 5 d. We found that DAMGO mimicked the morphine-induced increase in phospho-Src expression, suggesting that morphine signals through μ-receptors to drive Src kinase activation in microglia (Fig. 7*F*). Next, we examined whether Src is an intracellular mediator of the morphine-induced potentiation of P2X7R function in microglia. We tested the requirement for Src by using KBSrc4 (5 μM), which potently and selectively inhibits Src over other Src family kinases (Brandvold et al., 2012). KBSrc4 abrogated the increase in P2X7R-mediated currents in morphine-treated microglia (Fig. 7*C*,*D*). Thus, Src is a potential intracellular mediator of P2X7R and its activation by morphine is likely involved in the potentiation of P2X7R activity *in vitro*.

$Y_{382-384}$ is necessary for morphine potentiation of P2X7R activity

Having established that repeated morphine treatment activates Src kinase in microglia, and that Src kinase is necessary for enhanced receptor activity, we next examined potential tyrosine residues within the P2X7R required for this response to morphine treatment. We focused on tyrosine residue Y_{343} located in the putative second transmembrane domain of the P2X7R, and the intracellular C-terminus because of their known importance in regulating P2X7R activity (Surprenant et al., 1996; Kim et al., 2001). The P2X7R C-terminal domain is structurally unique among the P2X family of receptors and within this region; there

are 12 potential tyrosine residue sites. To identify the critical tyrosine residue(s) involved in morphine potentiation of P2X7R activity, we synthesized a library of palmitoylated small interfering peptides comprised of 10–14 aa that span specific tyrosine-containing regions within the P2X7R intracellular C-terminus, or that covered the Y_{343} containing region. Each of these membrane permeant peptides was coadministered with daily morphine in BV2 microglia culture (Fig. 8*A*). From this peptide screen, we found that only one palmitoylated peptide ($P2X7R_{379–389}$) containing a stretch of three tyrosine residues ($Y_{382–384}$) blocked the potentiation of P2X7R-mediated Ca^{2+} responses and currents (Fig. 8*A–C*). We also tested a control inactive peptide ($iP2X7R_{379–389}$) with identical amino acid composition, but with the $Y_{382–384}$ mutated to non-phosphorylatable phenylalanine residues ($Y_{382–384}F$). Treatment with the control phenylalanine containing peptide had no effect on the morphine-induced increase in P2X7R activity (Fig. 8*A*, *C*).

We reasoned that the enhancement of microglial P2X7R activity could simply be mediated by increased P2X7R cell-surface expression. To investigate whether morphine treatment affects P2X7R cell-surface expression, we biotinylated and isolated cell-surface proteins on BV2 microglia. Repeated morphine treatment significantly increased cell-surface P2X7R levels in microglia (Fig. 8*E*); this increase was concomitant with an increase in total P2X7R protein (Fig. 8*D*). Having identified $Y_{382–384}$ as a key regulatory site within the P2X7R, we next asked whether this site regulates P2X7R cell-surface expression. To target $Y_{382–384}$, we treated microglia in culture with the palmitoylated $P2X7R_{379–389}$ peptide, which did not prevent the morphine-induced upregulation of cell surface or total P2X7R protein levels (Fig. 8*D*, *E*). Our results indicate that in contrast to P2X7R activity, P2X7R expression is not regulated by $Y_{382–384}$. Likewise, KBSrc4 inhibition of Src kinase, which we determined is a key intracellular mediator of P2X7R phosphorylation, had no effect on P2X7R protein levels in morphine-treated cells (Fig. 8*D*, *E*). From these findings, we conclude that the potentiation of P2X7R activity by morphine is critically mediated by $Y_{382–384}$ in microglial cultures, whereas the upregulation of P2X7R cell surface and total expression in microglia do not depend on this site.

To pinpoint whether $Y_{382–384}$ is required for the modulation of P2X7R activity by morphine, we generated two P2X7R constructs encoding the wild-type P2X7R and a mutant P2X7R containing $Y_{382–384}A$ amino acid substitutions. These constructs were fused to the gene encoding the red fluorescent protein mCherry and expressed in 1321N1 cells that lack endogenous P2 receptors but possess μ-receptors (Fam et al., 2003). In mCherry-expressing cells, we assessed P2X7R cation channel function by applying BzATP. In the absence of morphine treatment, we found that the BzATP-evoked rise in intracellular $[Ca^{2+}]$ was indistinguishable between the wild-type and $Y_{382–384}A$ mutant forms of P2X7R (Fig. 8*F*), showing that cation channel function remained intact in the mutant P2X7R. Moreover, these findings indicate that the $Y_{382–384}$ site does not control basal P2X7R activity. By contrast, repeated morphine treatment significantly enhanced BzATP-evoked Ca^{2+} responses in cells expressing wild-type P2X7R, but not in cells expressing mutant P2X7R (Fig. 8*F*). These data together suggest that $Y_{382–384}$ within the P2X7R intracellular C-terminus is required for morphine potentiation of P2X7R activity.

Targeting $Y_{382–384}$ attenuates morphine tolerance and suppresses spinal microglia activation

Our findings in microglia cell culture indicate that $Y_{382–384}$ modulates P2X7R response to morphine treatment. We next examined whether targeting $Y_{382–384}$ in spinal P2X7R affects morphine antinociception by intrathecally administering the $P2X7R_{379–389}$ mimetic peptide. Treatment with $P2X7R_{379–389}$, but not $iP2X7R_{379–389}$ peptide, significantly attenuated the decline in morphine antinociception (Fig. 9*C*) and partially preserved morphine analgesic potency (Fig. 9*D*), without affecting the acute time course or the peak antinociceptive response to a single dose of morphine (Fig. 9*A*) and without interfering with daily baseline thresholds (Fig. 9*B*).

Finally, we assessed whether the $P2X7R_{379–389}$ mimetic peptide altered morphine-induced changes in microglial reactivity. We found that intrathecal administration of $P2X7R_{379–389}$ decreased the number of amoeboid-like (reactive) microglia (Fig. 10*A*, *C*), prevented the upregulation of CD11b (Fig. 10*B*, *D*), and reduced the percentage of CD11b-positive cells that were colabeled with the mitotic cell marker, Ki67 (Fig. 10*B*, *E*). Thus, $Y_{382–384}$ within the P2X7R intracellular C-terminus is a key site for the morphine-induced activation of spinal microglia (Fig. 10*F*). From these collective results, we conclude that site-specific modulation of P2X7R activity by $Y_{382–384}$ is critically involved in the development of morphine tolerance.

Discussion

Here, we have discovered a novel site-specific mechanism by which potentiation of P2X7R activity in microglia produces morphine analgesic tolerance. The most parsimonious interpretation of our findings is that morphine acting on μ-receptor signals through Src family kinase to potentiate P2X7R activity in microglia. We identified $Y_{382–384}$ within the P2X7R C-terminal domain as a putative phosphorylation site required for morphine potentiation of P2X7R activity. The $Y_{382–384}$ site does not affect normal P2X7R function, but rather it is differentially modulated by chronic morphine treatment. Selectively targeting this site suppressed spinal microglia reactivity and attenuated the development of morphine analgesic tolerance. Together, our findings reveal that $Y_{382–384}$ site-specific modulation of P2X7R in microglia is a novel spinal determinant of morphine analgesic tolerance.

P2X7Rs are expressed predominantly on immune cells in central and peripheral tissues (Sim et al., 2004; Hughes et al., 2007; Volonté et al., 2012). In the spinal cord, we confirmed that P2X7Rs are highly expressed on CD11b-positive microglia. Increased P2X7R activity is a cardinal feature of reactive microglia and a central tenet of microglial activation in the adult CNS. Our findings provide direct evidence that chronic morphine treatment potentiates the activity of endogenous P2X7Rs in adult resident spinal microglia. The activation of P2X7R requires ATP, and with chronic morphine treatment there is a reported increase in ATP levels within the brain (Nasello et al., 1973). Whether this increase in response to morphine also occurs in the spinal dorsal horn is not known, but in this region the release of ATP possibly derives from various sources, including primary sensory terminals, neurons, or astrocytes (Fam et al., 2000; Bodin and Burnstock, 2001; Masuda et al., 2016). Morphine-evoked ATP release from these sources could therefore drive P2X7R activity and convert spinal microglia toward a hyperactive phenotype. The release of ATP may also engage P2X7R expressed on neurons and astrocytes (Donnelly-Roberts and Jarvis, 2007; Ficker et al., 2014; Gao et al., 2017). Although our findings indicate that spinal P2X7R expression is relatively low in CD11b-negative cells, and this ex-

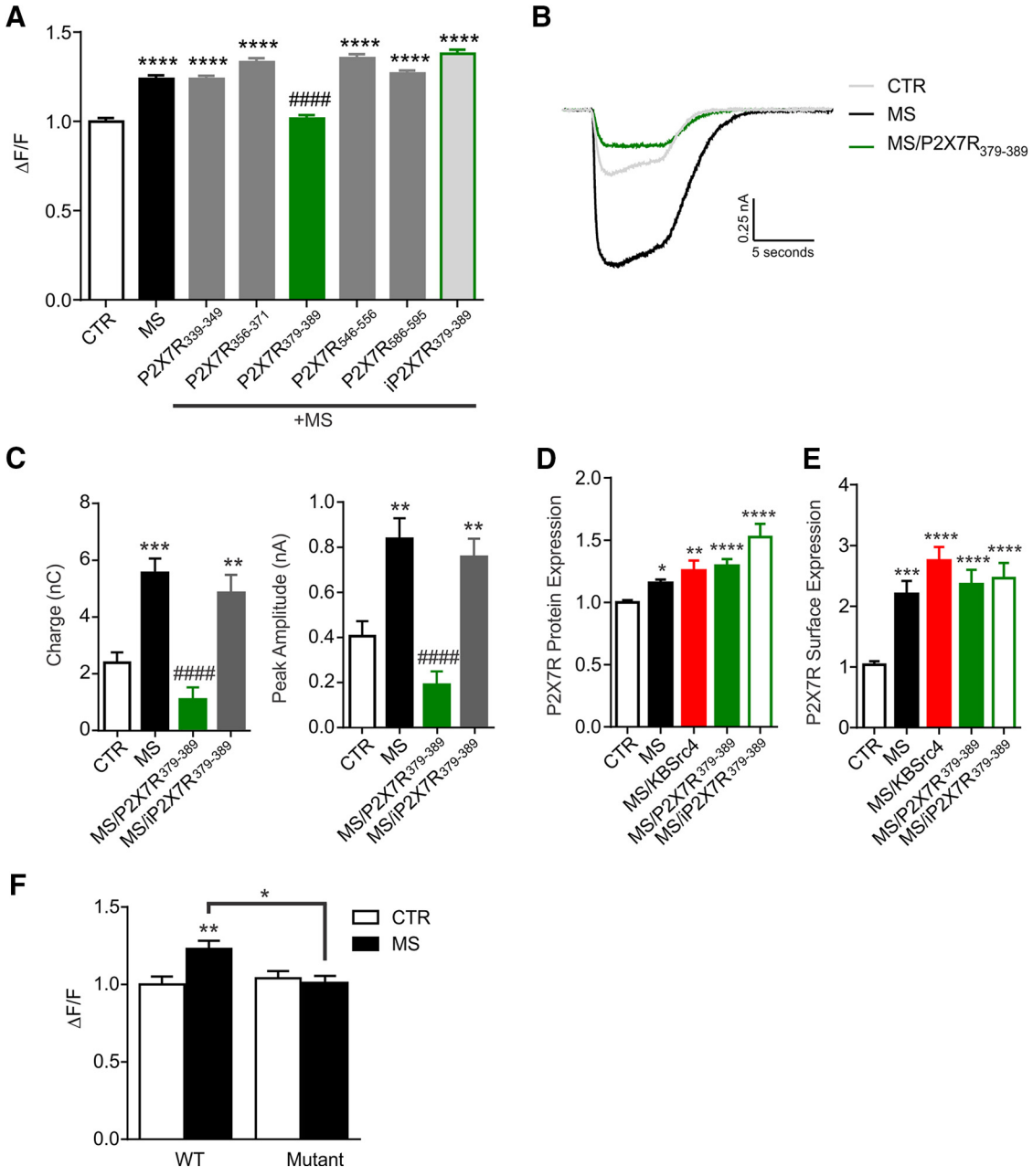

Figure 8. Morphine potentiation of P2X7R is modulated by C-terminal amino acid residues $Y_{382-384}$. ***A***, Palmitoylated peptides designed to mimic short regions of the P2X7R C-terminal domain or intracellular domains were administered (10 μM) to BV2 cells daily with MS to interfere with phosphorylation at these sites. Average $\Delta F/F$ of single-cell BzATP-evoked responses in BV2 microglia expressed relative to CTR. Palmitoylated peptide mimicking amino acids 379–389 of the C-terminal domain interfered with morphine-induced potentiation of BzATP-evoked P2X7R calcium responses. Cells were treated with MS (1 μM) and mimetic peptides ($n \sim 150$ cells, $n = 6–12$ plates). One-way ANOVA ($F_{(7,1471)} = 43.9$), Dunnett's *post hoc* test ($p < 0.0001$). ***B–E***, BV2 microglia were treated with the palmitoylated peptide containing amino acids spanning 379–389 of the P2X7R C-terminal domain, with an inactive control peptide with $Y_{382-384}F$ mutation. Peptides (10 μM) were coadministered in culture daily with morphine. ***B***, Representative tracings of the BzATP-evoked intracellular currents from cells treated with CTR, MS and $P2X7R_{379-389}$ or inactive peptide $iP2X7R_{379-389}$. ***C***, Average charge and peak amplitude for BzATP-evoked currents ($n = 9, 8, 6, 11$). CTR and MS groups same as shown in Figures 5*H*, 6*E*, and 7*D*. One-way ANOVA ($F_{(2,38)} = 15.4$; $F_{(3,31)} = 13.2$), Sidak's *post hoc* test (Charge: CTR vs MS: $p = 0.0008$; MS vs MS/$P2X7R_{379-389}$: $p < 0.0001$; CTR vs MS/$iP2X7R_{379-389}$: $p = 0.0053$; Peak: CTR vs MS: $p = 0.0021$; MS vs MS/$P2X7R_{379-389}$: $p < 0.0001$; CTR vs MS/$iP2X7R_{379-389}$: $p = 0.0093$). ***D***, Total P2X7R protein expression is increased in BV2 microglia treated with MS (1 μM; $n = 32$) and KBSrc4 (5 μM; $n = 14$), $P2X7R_{379-389}$ (10 μM; $n = 27$), or $iP2X7R_{379-389}$ (10 μM; $n = 13$) for 5 d compared with CTR ($n = 31$). One-way ANOVA ($F_{(4,112)} = 12.9$), Dunnett's *post hoc* test (CTR vs MS: $p = 0.417$; CTR vs MS/KBSrc4: $p = 0.0049$; CTR vs MS/$P2X7R_{379-389}$: $p < 0.0001$; MS vs MS/$iP2X7R_{379-389}$: $p < 0.0001$). ***E***, Cell-surface expression of P2X7R is increased in BV2 microglia treated with MS (1 μM; $n = 20$) and KBSrc4 (5 μM; $n = 12$), $P2X7R_{379-389}$ (10 μM; $n = 16$) or $iP2X7R_{379-389}$ (10 μM; $n = 15$) for 5 d compared with CTR ($n = 21$). One-way ANOVA ($F_{(4,79)} = 11.6$), Dunnett's *post hoc* test (CTR vs MS: $p = 0.0001$; CTR vs MS/KBSrc4: $p < 0.0001$; CTR vs MS/$P2X7R_{379-389}$: $p < 0.0001$; MS vs MS/$iP2X7R_{379-389}$: $p < 0.0001$). ***F***, P2X7R WT and mutant ($Y_{382-384}F$) constructs were expressed in an astrocytoma cell line (1321) that does not express endogenous P2X7Rs. Transfected cells were treated with morphine (MS; 1 μM) or CTR five times over 3 d before imaging. Average $\Delta F/F$ of BzATP-evoked responses in transfected 1321 cells expressed relative to WT CTR ($n = 27–32$ cells). Two-way ANOVA (interaction: $F_{(1,111)} = 6.9$; P2X7R WT/mut: $F_{(1,111)} = 3.3$; treatment: $F_{(1,111)} = 4.1$), Tukey's *post hoc* test (WT/CTR vs WT/MS: $p = 0.0064$; Mutant/CTR vs Mutant/MS: $p = 0.9740$; WT/MS vs Mutant/MS: $p = 0.0127$). All data represent mean ± SEM. ****$p < 0.0001$, ***$p < 0.001$, **$p < 0.01$, *$p < 0.05$ compared with CTR; ####$p < 0.0001$, #$p < 0.05$ compared with MS.

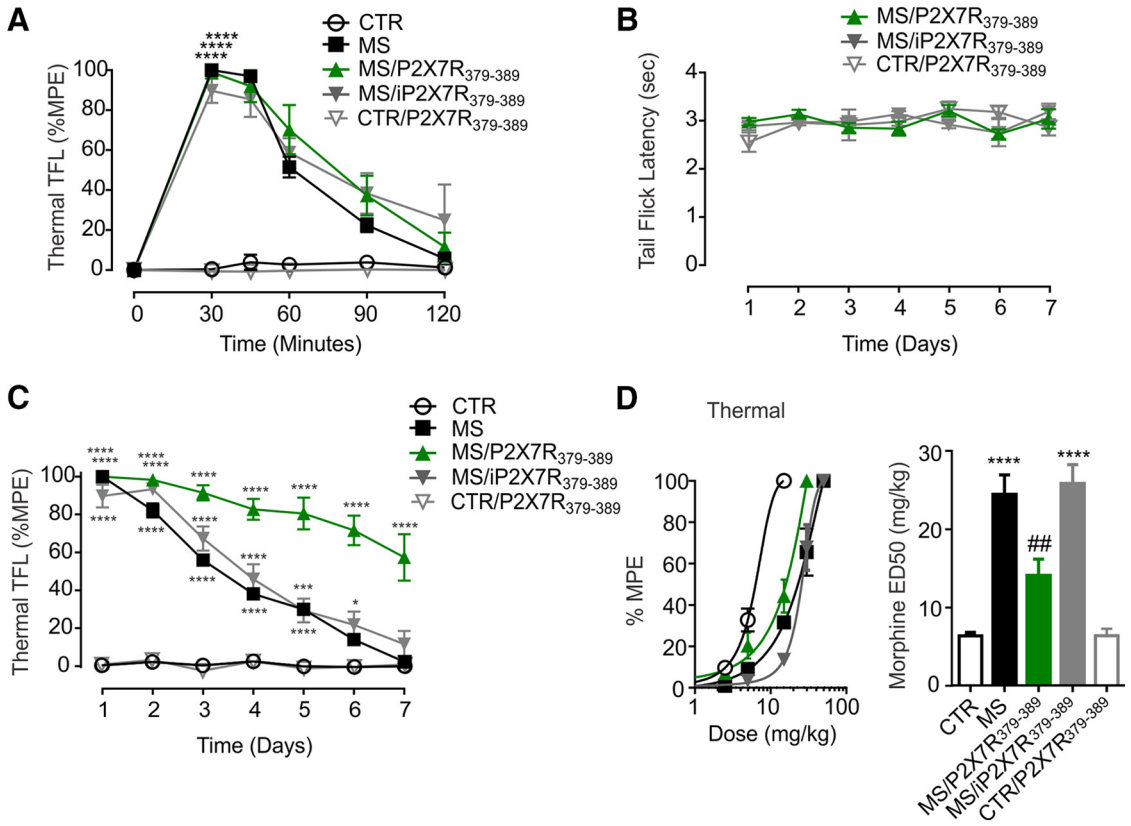

Figure 9. P2X7R Y382–384 gates the development of morphine tolerance in male rats. ***A–D***, Male Sprague-Dawley rats were treated with morphine (MS; 15 mg/kg i.p.) or saline as a control (CTR). Mimetic peptide $P2X7R_{379-389}$ (20 nM), inactive peptide (20 nM), or saline control (CTR) were injected into the intrathecal space. Morphine antinociception was assessed using thermal tail-flick (10 s cutoff). Latency to withdraw from stimulus [tail-flick latency (TFL)] is reported as a percentage of the maximum possible effect (MPE). ***A***, Acute anti-nociceptive response to first MS injection (15 mg/kg) in male rats. Repeated-measures two-way ANOVA, (interaction: $F_{(20,195)} = 16.18$; time: $F_{(5,195)} = 91.52$; treatment: $F_{(4,39)} = 60.14$; subjects: $F_{(39,195)} = 2.0$), Dunnett's *post hoc* test. ****$p < 0.0001$ compared with CTR at 30 min postinjection. ***B***, Daily raw thermal TFL baseline values in seconds before morphine injection. No change in baseline thresholds is observed with peptide treatment. ***C***, Daily thermal TFL in rats treated with MS (15 mg/kg; $n = 15$) with mimetic peptide $P2X7R_{379-389}$ (20 nM; $n = 9$) and inactive peptide (20 nM; $n = 8$) or CTR ($n = 5$) and CTR with mimetic peptide $P2X7R_{379-389}$ (20 nM; $n = 7$). Repeated-measures two-way ANOVA (interaction: $F_{(24,273)} = 13.73$; time: $F_{(6,273)} = 59.38$; treatment: $F_{(4,273)} = 351.8$), Dunnett's *post hoc* test. ****$p < 0.0001$, ***$p < 0.001$, *$p < 0.05$ compared with CTR on the same days. ***D***, Morphine dose–response curve and median effective dose (ED_{50}) of thermal TFL as measured on day 8 following 7 d treatment in male rats. CTR: 6.3 ± 0.4 mg/kg; MS: 24.2 ± 2.5 mg/kg; MS/ $P2X7R_{379-389}$:13.9 ± 2.1 mg/kg; MS/$iP2X7R_{379-389}$: 25.6 ± 2.4 mg/kg; CTR/$P2X7R_{379-389}$: 6.3 ± 0.9 mg/kg. One-way ANOVA ($F_{(4,24)} = 23.4$), Sidak's *post hoc* test (CTR vs MS: $p < 0.0001$; MS vs MS/$P2X7R_{379-389}$: $p = 0.0006$; CTR vs MS/$iP2X7R_{379-389}$: $p < 0.0001$). ****$p < 0.0001$ compared with CTR; ###$p < 0.001$ compared with MS. All data represent mean ± SEM.

pression is not impacted by morphine treatment, we cannot exclude the potential contribution of P2X7R from neurons and/or astrocytes in the development of morphine tolerance.

A key concept emerging from our study is that morphine causes site-specific potentiation of P2X7R in microglia. The intracellular C-terminal region of the P2X7R contains 12 potential tyrosine phosphorylation sites (Kim et al., 2001; Costa-Junior et al., 2011). We found that targeting $Y_{382–384}$ with an interfering peptide or directly mutating these tyrosine residues to non-phosphorylatable alanine prevented the potentiation of P2X7R-mediated currents or Ca^{2+} responses. These findings indicate that $Y_{382–384}$ is critical for morphine potentiation of P2X7R activity, and we surmise that $Y_{382–384}$ may be a putative tyrosine phosphorylation site that gates P2X7R cation channel function in response to morphine treatment. It is possible that phosphorylation of $Y_{382–384}$ is a key mechanistic step required for the phosphorylation of yet another site in the P2X7R. In addition, morphine may cause Src-dependent phosphorylation on a protein that closely associates with the P2X7R complex, and this in turn modulates receptor function through an interaction with $Y_{382–384}$. Little is known about the regulation of P2X7R activity by phosphorylation, and no prior study has reported $Y_{382–384}$ within the P2X7R as a putative phosphorylation site, or reported the impact of this site on P2X7R function, microglial reactivity, or its importance in the development of opioid tolerance.

Another potential explanation is that $Y_{382–384}$ regulates P2X7R cell-surface expression and the enhancement of P2X7R responses is simply due to altered expression. Although morphine treatment increased cell surface and total P2X7R protein levels, none of these receptor pools was affected by the $Y_{382–384}$ interfering peptide at a concentration that prevented the potentiation of P2X7R function, suggesting that the increase in P2X7R expression in and of itself cannot entirely account for the upregulation of P2X7R activity. Moreover, we determined in morphine naive cells and in in $Y_{382–384}$A mutant P2X7Rs, basal P2X7R currents and Ca^{2+} responses were unaffected by the $Y_{382–384}$ interfering peptide. $Y_{382–384}$ therefore has no bearing on normal P2X7R function, indicating that this site is differentially modulated by chronic morphine treatment. The unique functional selectivity of this site has important therapeutic implications because it allows for targeted inhibition of morphine-induced P2X7R activity, while leaving normal cation channel function of the receptor intact. The modulation of P2X7R cation channel function by tyrosine phosphorylation is not without precedent as Y_{343} and Y_{550} have been shown to affect basal P2X7R responses (Kim et al., 2001); however, we determined that

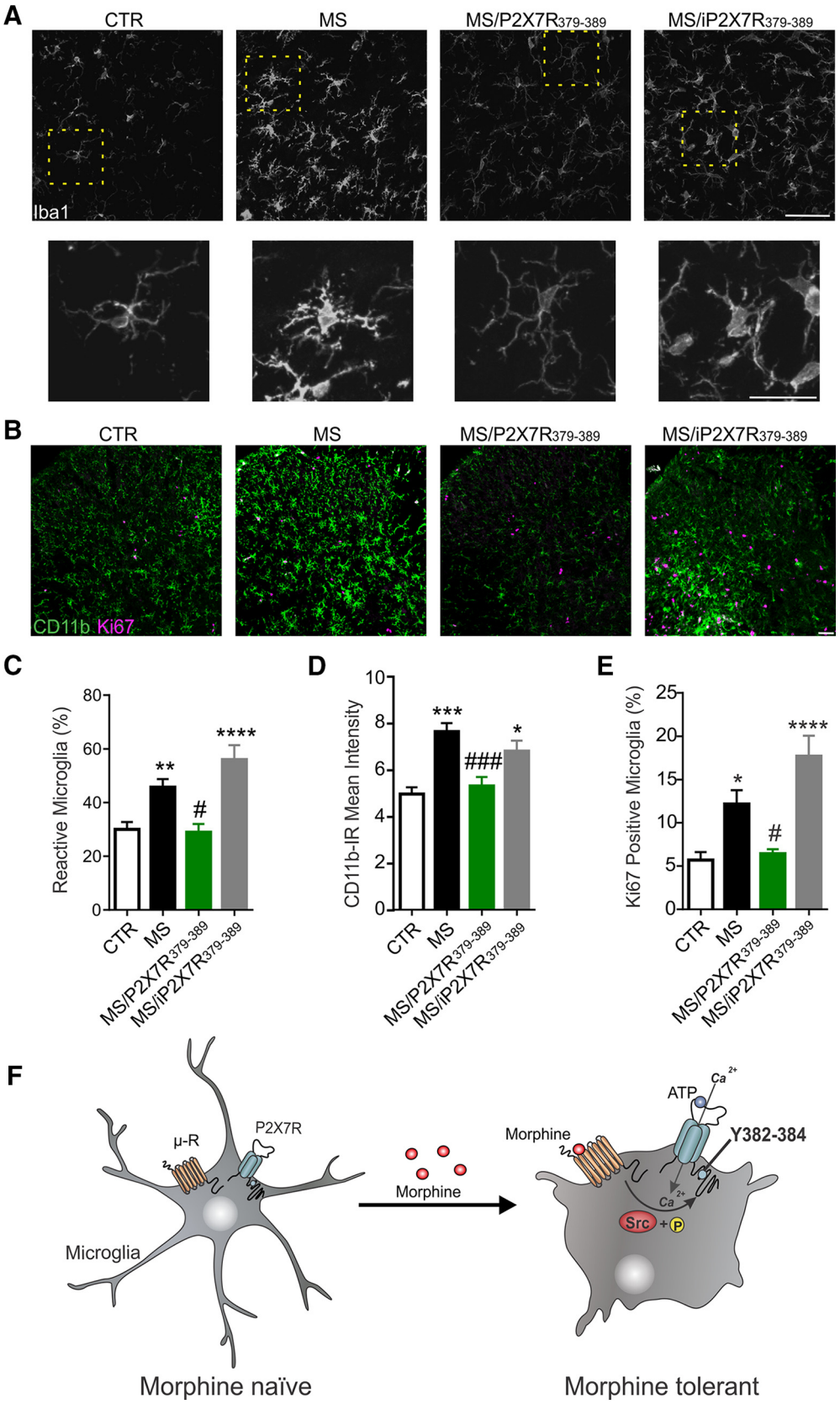

Figure 10. P2X7R Y382–384 modulates microglial reactivity in response to morphine. ***A***, Representative images of Iba1 expression in the spinal lumbar dorsal horn following 7 d of CTR or MS treatment with intrathecal injection of the P2X7R mimetic peptide ($P2X7R_{379-389}$; 20 nM) or its inactive control $iP2X7R_{379-389}$. Images were acquired at 60×. Scale bar, 50 μm. Yellow boxes represent area magnified three times to show representative microglial morphology. Scale bar, 25 μm. ***B***, Representative images of CD11b (green) and proliferation marker Ki67 (magenta) expression in the spinal lumbar dorsal horn following 7 d of CTR or MS treatment with intrathecal injection of the P2X7R mimetic peptide ($P2X7R_{379-389}$; 20 nM) or its inactive control $iP2X7R_{379-389}$. Images were acquired at 20×. Scale bar, 50 μm. ***C***, Morphology classification of Iba1-positive microglia in the lumbar dorsal horn. Microglia are qualitatively(*Figure legend continues.*)

these residues are not required for morphine potentiation of P2X7R activity in microglia.

Based on the pharmacological profiles of the inhibitors tested, we deduced that the effects of morphine on P2X7R activity are regulated by Src family kinases. In our search for the critical protein tyrosine kinase, we found that morphine treatment activates the non-receptor tyrosine kinase Src, and that inhibiting the activity of this kinase suppresses the increase in P2X7R activity. Together with the requirement for μ-receptors, a mechanistically simple interpretation is that morphine is acting on μ-receptor's signals to activate Src, which in turn enhances P2X7R function through a $Y_{382–384}$-dependent mechanism. Our data indicate that the increase in P2X7R activity and expression are μ-receptor dependent. There are, however, conflicting reports about the expression of μ-receptors on microglia (Börner et al., 2007; Turchan-Cholewo et al., 2008; Corder et al., 2017; Shrivastava et al., 2017). Here, we provide converging evidence for μ-receptor expression in spinal microglia. First, we show that CD11b and P2X7R coexpress with μ-receptors in adult rat spinal primary cell culture. We also detected μ-receptor transcripts in CD11b-positive cells isolated from adult spinal tissue by fluorescent activated cell sorting. We confirmed by PCR that the sorted cells indeed contain CD11b mRNA, but not GFAP or MAP2 mRNA. Finally, we also confirmed μ-receptor expression in BV2 microglia-like cell culture and primary microglia cultures isolated from the postnatal rat brain.

$Y_{382–384}$ contained in the P2X7R C-terminus is not within a Src consensus phosphorylation sequence, but it is nonetheless possible that Src might phosphorylate these tyrosine residues. Within the P2X7R complex, protein–protein interactions mediated by phosphorylation in the C-terminal domain are known to regulate cation channel function, localization, signaling, and cell-surface expression (Kim et al., 2001; Feng et al., 2005; Costa-Junior et al., 2011). Therefore, Src-dependent phosphorylation of P2X7R in response to morphine treatment could alter protein–protein interactions within the P2X7R complex: the loss or gain of these interactions may be permissive for increased P2X7R function.

Consistent with our findings in microglia cell culture, we determined *in vivo* that morphine treatment potentiates P2X7R function in resident spinal microglia. P2X7R activation in microglia drives proliferation and induces the switch from a resting to a reactive phenotype (Bianco et al., 2005; Monif et al., 2009); these responses are cellular correlates of microglia "activation" and are key features of morphine tolerance (Raghavendra et al., 2002; Kierdorf and Prinz, 2013). Intrathecal injection of the $Y_{382–384}$ interfering peptide blunted the morphine-induced upregulation of CD11b expression, suppressed microglia proliferation, and prevented the phenotypic switch to a hyperactive phenotype of microglia in the spinal dorsal horn. From these findings, we surmise that $Y_{382–384}$ is a specific locus within the P2X7R that modulates the microglial response to morphine treatment. Most striking was that the $Y_{382–384}$ interfering peptide also attenuated the progressive decline in morphine antinociception and preserved morphine analgesic potency, indicating that P2X7R activity mediated by $Y_{382–384}$ critically contributes to the development of morphine tolerance. Our findings therefore provide a missing mechanistic piece that links site-specific control of P2X7R function to the activation of spinal microglia and the development of morphine tolerance.

A downstream consequence of activating P2X7R on microglia is the release of cytokines, chemokines, and a host of other signaling molecules whose activity may compromise the analgesic response to morphine (Clark et al., 2010a,b; Chen et al., 2012). $Y_{382–384}$ may gate the P2X7R-mediated release of these signaling molecules that affect spinal microglia-to-neuron signaling in the development of morphine tolerance. Indeed, a complement of mechanisms in glia and neurons has been implicated in the development of opioid tolerance (Vanderah et al., 2001; Ossipov et al., 2005; Doyle et al., 2013). Whether these diverse mechanisms are causally linked through convergent or divergent pathways that modulate opioid analgesia are not known. Although TLR4 activation is one such mechanism that has been identified in microglia (Hutchinson et al., 2010), our results do not support a role for this receptor in the potentiation of P2X7R function by morphine. Rather, our data indicate that the μ-receptor is a critical signaling hub through which morphine enhances P2X7R function. The divergence between μ-receptor and TLR4 actions is supported by recent studies that have not confirmed a role for TLR4 in morphine tolerance, dependence, hyperalgesia, or reward (Fukagawa et al., 2013; Stevens et al., 2013; Mattioli et al., 2014; Skolnick et al., 2014). Because we found that spinal microglia are causally involved in the development, but not maintenance of analgesic tolerance, we surmise that microglia are the cellular "triggers" that oppose the pain-relieving effects of morphine and that potentiated P2X7R activity is a key mechanistic step through which morphine engages the microglia response.

In summary, our findings reveal that site-specific regulation of P2X7R in microglia is a key spinal determinant of morphine tolerance. We showed that $Y_{382–384}$ within the P2X7R is critically involved in the development of morphine tolerance. Of particular importance for therapeutic development, we found that targeting $Y_{382–384}$ preferentially blocks morphine potentiation of P2X7R function while leaving basal P2X7R function intact. Thus, a focused therapeutic strategy directed specifically against the $Y_{382–384}$ site might improve the long-term utility of morphine in treating pain, and produce fewer side effects than the indiscriminate inhibition of P2X7R. The ongoing struggle for control of pain complicates many conditions including cancer, stroke, diabetes, traumatic injury, and a host of other diseases. The implications of our findings may therefore extend to a diversity of disorders in which morphine and other opiates are the drugs of choice for optimal pain management.

←

(*Figure legend continued.*) assessed for process length, process thickness, number of processes, and cell body size. Individual cells are then classified as resting, intermediate, or activated. The percentage of each cell classification is then calculated per section and averaged across all sections ($n = 36, 22, 22, 21$). One-way ANOVA ($F_{(3,85)} = 12.9$), Sidak's *post hoc* test (CTR vs MS: $p = 0.0057$; MS vs MS/P2X7R$_{379–389}$: $p = 0.0157$; CTR vs MS/iP2X7R$_{379–389}$: $p < 0.0001$). ***D***, CD11b mean intensity from dorsal horn sections of the lumbar spinal cord ($n = 9, 12, 16, 13$). One-way ANOVA ($F_{(3,46)} = 9.6$), Sidak's *post hoc* test (CTR vs MS: $p = 0.0004$; MS vs MS/P2X7R$_{379–389}$: $p = 0.0003$; CTR vs MS/iP2X7R$_{379–389}$: $p < 0.0190$). ***E***, Percentage of microglia expressing the proliferation marker Ki67 out of all CD11b-positive cells in the field-of-view in the spinal dorsal horn from lumbar sections ($n = 9, 11, 14, 12$) taken from CTR-, MS-, MS/P2X7R$_{379–389}$-, and MS/iP2X7R$_{379–389}$-treated animals. One-way ANOVA ($F_{(3,42)} = 13.4$), Sidak's *post hoc* test (CTR vs MS: $p = 0.0329$; MS vs MS/P2X7R$_{379–389}$: $p = 0.0358$; CTR vs MS/iP2X7R$_{379–389}$: $p < 0.0001$). All data represent mean ± SEM. ****$p < 0.0001$, ***$p < 0.001$, **$p < 0.01$, *$p < 0.05$ compared with CTR; ###$p < 0.001$, ##$p < 0.01$, #$p < 0.05$ compared with MS. ***F***, Summary: potentiation of P2X7R activity in microglia is required for morphine analgesic tolerance. Morphine signaling through μ-receptors activates Src kinase in microglia. The activation of Src is a key intracellular substrate for morphine-induced enhancement of P2X7R function in microglia. This potentiated function depends on tyrosine residues $Y_{382–384}$ located within the P2X7R intracellular C-terminal domain. Site-specific P2X7R phosphorylation is critically required for morphine-induced microglial activation, and it is a novel mechanism in the development of morphine analgesic tolerance.

References

Bianchi BR, Lynch KJ, Touma E, Niforatos W, Burgard EC, Alexander KM, Park HS, Yu H, Metzger R, Kowaluk E, Jarvis MF, van Biesen T (1999) Pharmacological characterization of recombinant human and rat P2X receptor subtypes. Eur J Pharmacol 376:127–138. CrossRef Medline

Bianco F, Pravettoni E, Colombo A, Schenk U, Möller T, Matteoli M, Verderio C (2005) Astrocyte-derived ATP induces vesicle shedding and IL-1β release from microglia. J Immunol 174:7268–7277. CrossRef Medline

Bodin P, Burnstock G (2001) Purinergic signalling: ATP release. Neurochem Res 26:959–969. CrossRef Medline

Börner C, Stumm R, Höllt V, Kraus J (2007) Comparative analysis of mu-opioid receptor expression in immune and neuronal cells. J Neuroimmunol 188:56–63. CrossRef Medline

Brandvold KR, Steffey ME, Fox CC, Soellner MB (2012) Development of a highly selective c-Src kinase inhibitor. ACS Chem Biol 7:1393–1398. CrossRef Medline

Brown MT, Cooper JA (1996) Regulation, substrates and functions of src. Biochim Biophys Acta 1287:121–149. CrossRef Medline

Burma NE, Bonin RP, Leduc-Pessah H, Baimel C, Cairncross ZF, Mousseau M, Shankara JV, Stemkowski PL, Baimoukhametova D, Bains JS, Antle MC, Zamponi GW, Cahill CM, Borgland SL, De Koninck Y, Trang T (2017a) Blocking microglial pannexin-1 channels alleviates morphine withdrawal in rodents. Nat Med 23:355–360. CrossRef Medline

Burma NE, Leduc-Pessah H, Trang T (2017b) Genetic deletion of microglial Panx1 attenuates morphine withdrawal, but not analgesic tolerance or hyperalgesia in mice. Channels (Austin) 1–8. CrossRef Medline

Cai Y, Kong H, Pan YB, Jiang L, Pan XX, Hu L, Qian YN, Jiang CY, Liu WT (2016) Procyanidins alleviates morphine tolerance by inhibiting activation of NLRP3 inflammasome in microglia. J Neuroinflammation 13:53. CrossRef Medline

Chen ML, Cao H, Chu YX, Cheng LZ, Liang LL, Zhang YQ, Zhao ZQ (2012) Role of P2X7 receptor-mediated IL-18/IL-18R signaling in morphine tolerance: multiple glial-neuronal dialogues in the rat spinal cord. J Pain 13:945–958. CrossRef Medline

Clark AK, Wodarski R, Guida F, Sasso O, Malcangio M (2010a) Cathepsin S release from primary cultured microglia is regulated by the P2X7 receptor. Glia 58:1710–1726. CrossRef Medline

Clark AK, Staniland AA, Marchand F, Kaan TK, McMahon SB, Malcangio M (2010b) P2X7-dependent release of interleukin-1β and nociception in the spinal cord following lipopolysaccharide. J Neurosci 30:573–582. CrossRef Medline

Corder G, Tawfik VL, Wang D, Sypek EI, Low SA, Dickinson JR, Sotoudeh C, Clark JD, Barres BA, Bohlen CJ, Scherrer G (2017) Loss of μ opioid receptor signaling in nociceptors, but not microglia, abrogates morphine tolerance without disrupting analgesia. Nat Med 23:164–173. CrossRef Medline

Costa-Junior HM, Sarmento Vieira F, Coutinho-Silva R (2011) C terminus of the P2X7 receptor: treasure hunting. Purinergic Signal 7:7–19. CrossRef Medline

D'Amour FE, Smith DL (1941) A method for determining loss of pain sensation. J Pharmacol Exp Ther 72:74–79.

De la Calle JL, Paíno CL (2002) A procedure for direct lumbar puncture in rats. Brain Res Bull 59:245–250. CrossRef Medline

Donnelly-Roberts DL, Jarvis MF (2007) Discovery of P2X7 receptor-selective antagonists offers new insights into P2X7 receptor function and indicates a role in chronic pain states. Br J Pharmacol 151:571–579. Medline

Doyle T, Esposito E, Bryant L, Cuzzocrea S, Salvemini D (2013) NADPH-oxidase 2 activation promotes opioid-induced antinociceptive tolerance in mice. Neuroscience 241:1–9. CrossRef Medline

Fam SR, Gallagher CJ, Salter MW (2000) P2Y1 purinoceptor-mediated Ca2+ signaling and Ca2+ wave propagation in dorsal spinal cord astrocytes. J Neurosci 20:2800–2808. Medline

Fam SR, Gallagher CJ, Kalia LV, Salter MW (2003) Differential frequency dependence of P2Y1- and P2Y2-mediated Ca 2+ signaling in astrocytes. J Neurosci 23:4437–4444. Medline

Feng YH, Wang L, Wang Q, Li X, Zeng R, Gorodeski GI (2005) ATP stimulates GRK-3 phosphorylation and β-arrestin-2-dependent internalization of P2X7 receptor. Am J Physiol Cell Physiol 288:C1342–C1356. CrossRef Medline

Ferrini F, Trang T, Mattioli TA, Laffray S, Del'Guidice T, Lorenzo LE, Castonguay A, Doyon N, Zhang W, Godin AG, Mohr D, Beggs S, Vandal K, Beaulieu JM, Cahill CM, Salter MW, De Koninck Y (2013) Morphine hyperalgesia gated through microglia-mediated disruption of neuronal Cl− homeostasis. Nat Neurosci 16:183–192. CrossRef Medline

Ficker C, Rozmer K, Kató E, Andó RD, Schumann L, Krügel U, Franke H, Sperlágh B, Riedel T, Illes P (2014) Astrocyte-neuron interaction in the substantia gelatinosa of the spinal cord dorsal horn via P2X7 receptor-mediated release of glutamate and reactive oxygen species. Glia 62:1671–1686. CrossRef Medline

Fukagawa H, Koyama T, Kakuyama M, Fukuda K (2013) Microglial activation involved in morphine tolerance is not mediated by toll-like receptor 4. J Anesth 27:93–97. CrossRef Medline

Gao J, Zhang T, Kang Z, Ting W, Xu L, Yin D (2017) The F0F1 ATP synthase regulates human neutrophil migration through cytoplasmic proton extrusion coupled with ATP generation. Mol Immunol 90:219–226. CrossRef Medline

Honore P, Donnelly-Roberts D, Namovic MT, Hsieh G, Zhu CZ, Mikusa JP, Hernandez G, Zhong C, Gauvin DM, Chandran P, Harris R, Medrano AP, Carroll W, Marsh K, Sullivan JP, Faltynek CR, Jarvis MF (2006) A-740003 [N-(1-{[(cyanoimino)(5-quinolinylamino) methyl]amino}-2,2-dimethylpropyl)-2-(3,4-dimethoxyphenyl)acetamide], a novel and selective P2X7 receptor antagonist, dose-dependently reduces neuropathic pain in the rat. J Pharmacol Exp Ther 319:1376–1385. CrossRef Medline

Hughes JP, Hatcher JP, Chessell IP (2007) The role of P2X7 in pain and inflammation. Purinergic Signal 3:163–169. CrossRef Medline

Hutchinson MR, Coats BD, Lewis SS, Zhang Y, Sprunger DB, Rezvani N, Baker EM, Jekich BM, Wieseler JL, Somogyi AA, Martin D, Poole S, Judd CM, Maier SF, Watkins LR (2008) Proinflammatory cytokines oppose opioid-induced acute and chronic analgesia. Brain Behav Immun 22:1178–1189. CrossRef Medline

Hutchinson MR, Zhang Y, Shridhar M, Evans JH, Buchanan MM, Zhao TX, Slivka PF, Coats BD, Rezvani N, Wieseler J, Hughes TS, Landgraf KE, Chan S, Fong S, Phipps S, Falke JJ, Leinwand LA, Maier SF, Yin H, Rice KC, Watkins LR (2010) Evidence that opioids may have toll-like receptor 4 and MD-2 effects. Brain Behav Immun 24:83–95. CrossRef Medline

Hutchinson MR, Shavit Y, Grace PM, Rice KC, Maier SF, Watkins LR (2011) Exploring the neuroimmunopharmacology of opioids: an integrative review of mechanisms of central immune signaling and their implications for opioid analgesia. Pharmacol Rev 63:772–810. CrossRef Medline

Iwaszkiewicz KS, Schneider JJ, Hua S (2013) Targeting peripheral opioid receptors to promote analgesic and anti-inflammatory actions. Front Pharmacol 4:132. CrossRef Medline

Jarvis MF (2010) The neural-glial purinergic receptor ensemble in chronic pain states. Trends Neurosci 33:48–57. CrossRef Medline

Kierdorf K, Prinz M (2013) Factors regulating microglia activation. Front Cell Neurosci 7:44. CrossRef Medline

Kim M, Jiang LH, Wilson HL, North RA, Surprenant A (2001) Proteomic and functional evidence for a P2X7 receptor signalling complex. EMBO J 20:6347–6358. CrossRef Medline

Levitzki A, Gazit A (1995) Tyrosine kinase inhibition: an approach to drug development. Science 267:1782–1788. CrossRef Medline

Masuda T, Ozono Y, Mikuriya S, Kohro Y, Tozaki-Saitoh H, Iwatsuki K, Uneyama H, Ichikawa R, Salter MW, Tsuda M, Inoue K (2016) Dorsal horn neurons release extracellular ATP in a VNUT-dependent manner that underlies neuropathic pain. Nat Commun 7:12529. CrossRef Medline

Mattioli TA, Leduc-Pessah H, Skelhorne-Gross G, Nicol CJ, Milne B, Trang T, Cahill CM (2014) Toll-like receptor 4 mutant and null mice retain morphine-induced tolerance, hyperalgesia, and physical dependence. PloS One 9:e97361. CrossRef Medline

Mayer DJ, Mao J, Holt J, Price DD (1999) Cellular mechanisms of neuropathic pain, morphine tolerance, and their interactions. Proc Natl Acad Sci U S A 96:7731–7736. CrossRef Medline

McNaull B, Trang T, Sutak M, Jhamandas K (2007) Inhibition of tolerance to spinal morphine antinociception by low doses of opioid receptor antagonists. Eur J Pharmacol 560:132–141. CrossRef Medline

Mika J, Wawrzczak-Bargiela A, Osikowicz M, Makuch W, Przewlocka B (2009) Attenuation of morphine tolerance by minocycline and pentoxifylline in naive and neuropathic mice. Brain Behav Immun 23:75–84. CrossRef Medline

Monif M, Reid CA, Powell KL, Smart ML, Williams DA (2009) The P2X7 receptor drives microglial activation and proliferation: a trophic role for P2X7R pore. J Neurosci 29:3781–3791. CrossRef Medline

Nasello AG, Depiante R, Tannhauser M, Izquierdo I (1973) Effect of mor-

phine on the RNA and ATP concentration of brain structures of the rat. Pharmacology 10:56–59. CrossRef Medline

Onogi T, Minami M, Katao Y, Nakagawa T, Aoki Y, Toya T, Katsumata S, Satoh M (1995) DAMGO, a μ-opioid receptor selective agonist, distinguishes between μ- and δ-opioid receptors around their first extracellular loops. FEBS Lett 357:93–97. CrossRef Medline

Ossipov MH, Lai J, King T, Vanderah TW, Porreca F (2005) Underlying mechanisms of pronociceptive consequences of prolonged morphine exposure. Biopolymers 80:319–324. CrossRef Medline

Raghavendra V, Rutkowski MD, DeLeo JA (2002) The role of spinal neuroimmune activation in morphine tolerance/hyperalgesia in neuropathic and sham-operated rats. J Neurosci 22:9980–9989. Medline

Rettinger J, Schmalzing G (2004) Desensitization masks nanomolar potency of ATP for the P2X1 receptor. J Biol Chem 279:6426–6433. CrossRef Medline

Riazi K, Galic MA, Kuzmiski JB, Ho W, Sharkey KA, Pittman QJ (2008) Microglial activation and TNFalpha production mediate altered CNS excitability following peripheral inflammation. Proc Natl Acad Sci U S A 105:17151–17156. CrossRef Medline

Rivat C, Sebaihi S, Van Steenwinckel J, Fouquet S, Kitabgi P, Pohl M, Melik Parsadaniantz S, Reaux-Le Goazigo A (2014) Src family kinases involved in CXCL12-induced loss of acute morphine analgesia. Brain Behav Immun 38:38–52. CrossRef Medline

Shrivastava P, Cabrera MA, Chastain LG, Boyadjieva NI, Jabbar S, Franklin T, Sarkar DK (2017) Mu-opioid receptor and delta-opioid receptor differentially regulate microglial inflammatory response to control proopiomelanocortin neuronal apoptosis in the hypothalamus: effects of neonatal alcohol. J Neuroinflammation 14:83. CrossRef Medline

Sim JA, Young MT, Sung HY, North RA, Surprenant A (2004) Reanalysis of P2X7 receptor expression in rodent brain. J Neurosci 24:6307–6314. CrossRef Medline

Skolnick P, Davis H, Arnelle D, Deaver D (2014) Translational potential of naloxone and naltrexone as TLR4 antagonists. Trends Pharmacol Sci 35:431–432. CrossRef Medline

Song P, Zhao ZQ (2001) The involvement of glial cells in the development of morphine tolerance. Neurosci Res 39:281–286. CrossRef Medline

Stevens CW, Aravind S, Das S, Davis RL (2013) Pharmacological characterization of LPS and opioid interactions at the toll-like receptor 4. Br J Pharmacol 168:1421–1429. CrossRef Medline

Surprenant A, Rassendren F, Kawashima E, North RA, Buell G (1996) The cytolytic P2Z receptor for extracellular ATP identified as a P2X receptor (P2X7). Science 272:735–738. CrossRef Medline

Sweitzer S, De Leo J (2011) Propentofylline: glial modulation, neuroprotection, and alleviation of chronic pain. Handb Exp Pharmacol 200:235–250. CrossRef Medline

Trang T, Beggs S, Wan X, Salter MW (2009) P2X4-receptor-mediated synthesis and release of brain-derived neurotrophic factor in microglia is dependent on calcium and p38-mitogen-activated protein kinase activation. J Neurosci 29:3518–3528. CrossRef Medline

Turchan-Cholewo J, Dimayuga FO, Ding Q, Keller JN, Hauser KF, Knapp PE, Bruce-Keller AJ (2008) Cell-specific actions of HIV-Tat and morphine on opioid receptor expression in glia. J Neurosci Res 86:2100–2110. CrossRef Medline

Vanderah TW, Suenaga NM, Ossipov MH, Malan TP Jr, Lai J, Porreca F (2001) Tonic descending facilitation from the rostral ventromedial medulla mediates opioid-induced abnormal pain and antinociceptive tolerance. J Neurosci 21:279–286. Medline

Volonté C, Apolloni S, Skaper SD, Burnstock G (2012) P2X7 receptors: channels, pores and more. CNS Neurol Disord Drug Targets 11:705–721. CrossRef Medline

Watkins LR, Hutchinson MR, Johnston IN, Maier SF (2005) Glia: novel counter-regulators of opioid analgesia. Trends Neurosci 28:661–669. CrossRef Medline

Wen YR, Tan PH, Cheng JK, Liu YC, Ji RR (2011) Microglia: a promising target for treating neuropathic and postoperative pain, and morphine tolerance. J Formos Med Assoc Taiwan Yi Zhi 110:487–494. CrossRef Medline

Yip PK, Kaan TK, Fenesan D, Malcangio M (2009) Rapid isolation and culture of primary microglia from adult mouse spinal cord. J Neurosci Methods 183:223–237. CrossRef Medline

Zhang L, Zhao H, Qiu Y, Loh HH, Law PY (2009) Src phosphorylation of μ-receptor is responsible for the receptor switching from an inhibitory to a stimulatory signal. J Biol Chem 284:1990–2000. CrossRef Medline

Zhang L, Loh HH, Law PY (2013) A novel noncanonical signaling pathway for the μ-opioid receptor. Mol Pharmacol 84:844–853. CrossRef Medline

Zhao YL, Chen SR, Chen H, Pan HL (2012) Chronic opioid potentiates presynaptic but impairs postsynaptic *N*-methyl-D-aspartic acid receptor activity in spinal cords: implications for opioid hyperalgesia and tolerance. J Biol Chem 287:25073–25085. CrossRef Medline

Zhou D, Chen ML, Zhang YQ, Zhao ZQ (2010) Involvement of spinal microglial P2X7 receptor in generation of tolerance to morphine analgesia in rats. J Neurosci 30:8042–8047. CrossRef Medline